FEDERAL UNIVERSITY OF TECHNOLOGY - PARANÁ
GRADUATE PROGRAM IN ELECTRICAL AND COMPUTER ENGINEERING

DANIEL HAYASHIDA SIMÃO

ENERGY EFFICIENCY OF MULTI-HOP UNDERWATER ACOUSTIC NETWORKS USING FOUNTAIN CODES

THESIS

CURITIBA
2021

DANIEL HAYASHIDA SIMÃO

ENERGY EFFICIENCY OF MULTI-HOP UNDERWATERACOUSTIC NETWORKS USING FOUNTAIN CODES

Eficiência energética em redes acústicas subaquáticas considerando múltiplos saltos e usando códigos de fontanais

Tese apresentada como requisito para obtenção do título de Doutor em Ciência, do Programa de Pós-Graduação em Engenharia Elétrica e Informática Industrial, da Universidade Tecnológica Federal do Paraná(UTFPR).

Orientador: Prof. Dr. Glauber Gomes de Oliveira Brante

Coorientador: Prof. Dr. Bruno Sens Chang

CURITIBA

2021

Ministério da Educação
Universidade Tecnológica Federal do Paraná
Campus Curitiba

DANIEL HAYASHIDA SIMAO

ENERGY EFFICIENCY OF MULTI-HOP UNDERWATER ACOUSTIC NETWORKS USING FOUNTAIN CODES

Trabalho de pesquisa de doutorado apresentado como requisito para obtenção do título de Doutor Em Ciências da Universidade Tecnológica Federal do Paraná (UTFPR). Área de concentração: Telecomunicações E Redes.

Data de aprovação: 27 de Agosto de 2021

Prof Glauber Gomes De Oliveira Brante, Doutorado - Universidade Tecnológica Federal do Paraná

Prof Hermes Irineu Del Monego, Doutorado - Universidade Tecnológica Federal do Paraná

Prof Joao Luiz Rebelatto, Doutorado - Universidade Tecnológica Federal do Paraná

Prof Marcelo Eduardo Pellenz, Doutorado - Pontifícia Universidade Católica do Paraná (Pucpr)

Prof Marcos Tomio Kakitani, Doutorado - Universidade Federal de São João Del Rei (Ufsj)

Documento gerado pelo Sistema Acadêmico da UTFPR a partir dos dados da Ata de Defesa em 27/08/2021.

I would like to dedicate this work to all the peoples who helped me and believed in me.

ACKNOWLEDGMENTS

I would like to thank my supervisors, Dr. Glauber Brante and Dr. Bruno Chang, for their patience, guidance and support. I benefited greatly from their wealth of knowledge and invaluable experience. I am very proud to be your student.

I thank Federal University of Technology - Paraná for providing all the conditions to complete this project, as well as all the teachers and reviewers who contributed with the work.

I thank my wife, Ana Laura, whose constant love and support keep me motivated and confident. My accomplishments and success are because she believed in me.

I thank my adorable pet, Kira.

And finally, I thank my family who supported this long process with me, always offering support and love.

RESUMO

SIMÃO, Daniel. **Energy Efficiency of Multi-Hop Underwater Acoustic Networks Using Fountain Codes**. 2021. 54 f. THESIS (PhD in Electrical and Computer Engineering) – Federal University of Technology - Paraná, Curitiba, 2021.

Garantir o baixo consumo de energia é algo crucial nas comunicações subaquáticas, uma vez que a substituição da bateria dos sensores nesse cenário é algo indesejável devido à dificuldade e alto custo financeiro. No presente trabalho analisamos o consumo energético de uma rede acústica subaquática implementando códigos fontanais, algo que fornece uma característica interessante para cenários com longos atrasos de transmissão, como é o caso das redes acústicas subaquáticas. Assim, a otimização do número de pacotes redundantes em conjunto com a possibilidade de retransmissões a cada salto para garantir confiabilidade permitem uma otimização global da rede. Além disso, para reduzir o consumo de energia neste cenário, otimizamos a ordem de modulação assumindo um chaveamento de mudança de fase diferencial (M-DPSK), bem como o número de saltos e tentativas de transmissão por salto. Investigamos o número necessário de pacotes codificados por fonte para diferentes ordens de modulação e número de saltos. Nossos resultados mostram que, ao permitir retransmissões e otimizar o número de saltos e a ordem de modulação, podemos obter importantes economias de energia, principalmente em cenários de longas distâncias. Além disso, com códigos fontanais, o consumo de energia diminui significativamente em comparação com o caso sem códigos fontanais, permitindo até 40% de economia.

Palavras-chave: Redes Subaquáticas, Eficiência Energética, Consumo de Energia, Canal Acústico, Códigos Corretores de Erros, Códigos Fontanais.

ABSTRACT

SIMÃO, Daniel. **Energy Efficiency of Multi-Hop Underwater Acoustic Networks Using Fountain Codes**. 2021. 54 f. THESIS (PhD in Electrical and Computer Engineering) – Federal University of Technology - Paraná, Curitiba, 2021.

Ensuring low energy consumption is a crucial issue in underwater communications, since battery replacement may be difficult and expensive in these scenarios. In this work we analyze the energy consumption of a multi-hop underwater acoustic network (UWAN) employing fountain codes, which provides an interesting feature to scenarios with long transmission delays, as is the case of UWANs. Thus, the proper optimization of the number of redundant packets as well as the possibility of retransmissions per hop in order to ensure reliability allows a global optimization of the network. Moreover, in order to reduce the energy consumption in this scenario we optimize the modulation order assuming differential phase-shift keying (M-DPSK), as well as the number of hops and transmission trials per hop. We investigate the required number of fountain-encoded packets for different modulation orders and number of hops. Our results show that, by allowing retransmissions and optimizing the number of hops and the modulation order, we can obtain important energy savings, especially for long distances. In addition, with fountain codes the energy consumption decreases significantly compared to the case without fountain codes, allowing up to 40% of savings.

Keywords: Underwater Networks, Energy Efficiency, Energy Consumption, Acoustic Channel, Error-Correcting Codes, Fountain Codes.

LIST OF FIGURES

LIST OF TABLES

LIST OF ACRONYMS

APU	Arithmetic Processing Unit
ARQ	Automatic Repeat Request
BCH	Bose-Chaudhuri-Hocquenghem
BER	Bit error rate
DCA	Convex Difference Algorithm
DPSK	Differential Phase Shift Keying
DSA	Discrete Stochastic Approximation
FEC	Forward Error Correction
FER	Frame error rate
HARQ	Hybrid Automatic Repeat Request
IoT	Internet of Things
IoUT	Internet of Underwater Things
JPR	Joint Power and Rate Control
OFDM	Orthogonal Frequency Division Multiplexing
PAPR	Peak-to-Average Power Ratio
PSD	Power spectral density
QoS	Quality of Service
RF	Radio-frequency
SNR	Signal-to-noise Ratio
UWANs	Underwater acoustic networks

LIST OF SYMBOLS

M	Modulation order
l	Link distance
φ	Number of hops
τ	Number of transmission trials
A_0	Unit-normalizing Constant
κ	Propagation Geometry
f	Frequency
$a(f)$	Absorption Coefficient
N_{t}	Turbulence Noise
N_{s}	Transport Noise
N_{w}	Wave Noise
N_{th}	Thermal Noise
s	Shipping Activity Factors
w	Wind Speed
$N(f)$	Total Noise
M_l	Link Margin
B	Bandwidth
γ_k	Instantaneous SNR
$\overline{\gamma}_k$	Average SNR
h	Acoustic Channel Fading
$f_o(l_k)$	Optimal frequency
K	Parameter of the K-fading
ν	Shape parameter
ψ	Scale parameter
$K_{\nu-1}$	Modified Bessel Function of the Second Kind
$\Gamma(\nu)$	Gamma function
$P_b(\overline{\gamma}_k)$	BER of the M-DPSK considering a Rayleigh distribution
L	Payload
$P_{\mathrm{f}}(\overline{\gamma})$	Frame Error Rate
Z	Number of information packets
$P_s(\overline{\gamma}_k)$	The probability of success
Y	Number of coded packets
$P_{\mathrm{f}}^{\star}$	Target FER
$\beta(Y_{\mathrm{opt}}, \overline{\gamma}_k)$	Result of the optimization process
$\epsilon_{\mathrm{bT}}(\tau, \varphi)$	Total Energy Consumption
$\epsilon_{\mathrm{tx}}(\tau, \varphi)$	Energy Consumed by Each Transmitter
$\epsilon_{\mathrm{rx}}(\tau, \varphi)$	Energy Corresponding Feedback Bits
$P_{\mathrm{el,tx}}$	Power consumption of baseband operations at the transmitter
$P_{\mathrm{el,rx}}$	Power consumption at the receiver
P_{PA}	Power used by the power amplifier
T	Transmission time per payload bit

T_{f}	Feedback time per bit
R_b	Bit rate
F	Number of feedback bits
α	Peak-to-Average Power Ratio of the transmitted signal
ϕ	Overall efficiency of the power amplifier and transducer
P_{el}	Average total energy consumption
r	Code rate
$\hat{\epsilon}_{\mathrm{bT}}(\tau, \varphi)$	Total energy consumption using convolutional codes
ϵ_{enc}	Energy spent to encode each symbol
ϵ_{dec}	Energy spent to decode each symbol
J	Number of different types of arithmetic operations required for encoding
c_j	Number of clock cycles required by that operation
n_j	Number of times such operation is performed during the encoding/decoding algorithm
V_{dd}	APU operating voltage
I_0	Average current during the execution time of the arithmetic operations
f_{APU}	APU's clock frequency
H	Header bits
O	Overhead
$\hat{T}$	Transmission time
$\hat{T}_{\mathrm{f}}$	Feedback time per payload bit

SUMMARY

1 INTRODUCTION

Underwater acoustic networks (UWANs) are the basis of many applications involving tactical surveillance, coastline defense, off-shore production, ecological monitoring, scientific exploration, and disaster prevention (JIANG, 2018). Moreover, energy consumption is a crucial factor to be considered in the design and construction of the underwater devices. Since most devices are battery operated, replacement in underwater networks can be a challenge even greater that that in terrestrial networks (SOUZA et al., 2016a). In addition, electromagnetic waves used in terrestrial radio communications have poor performance in underwater environments, making acoustic waves a more interesting choice for communication in these scenarios (SOUZA et al., 2016a). However, unlike terrestrial wireless sensor networks, UWANs are characterized by limited available transmission power and bandwidth, and a harsh communication environment affected by a long channel propagation delay, large attenuation and time-varying channel conditions (XING, 2017).

Recently, many application options for Machine Learning and Internet of Things have been discussed, but this subject is not covered much in underwater environments, although 44% of the earth's oceans cover more than 70% of the earth's surface and 90% of international trades is done through nautical transportation. Therefore, underwater research and development could have a significant impact on many aspects of human's life by establishing and rolling out the Internet of Underwater Things (IoUT) (JAHANBAKHT et al., 2021). Some examples of applications were presented as IoUT tracking data: for vessel monitoring and marine accidents; Marine cartographic data: for essential naval data; protected and sensitive areas; Oceanic climate data: for nautical weather and satellite imagery; IoUT commerce data: for shipping companies and marine conservation organizations.

In order to obtain low energy consumption in underwater acoustic communications, in (SRIVASTAVA; KOKSAL, 2010) a scheduler that minimizes the number of transmission attempts and guarantees a given throughput constraint was proposed, whereas the heuristic scheduler proposed in (TOMASI; PREISIG, 2015) keeps attempting transmission until the queue is empty. The heuristics scheduler is based on a condition verification with threshold. An evaluation of the performance of these schedulers using real world data was done in (TOMASI; PREISIG, 2019); it was found out that the heuristic scheduler from (TOMASI; PREISIG, 2015) performs close to optimal at low and

medium-high throughput constraint, thus becoming a valuable algorithm for transmission scheduling in practical system.

Therefore, in order to improve performance in UWANs, it is important that the communication parameters are optimized. For instance, in (SOUZA et al., 2016b) the authors optimize the code rate of a convolutional encoder, the signal-to-noise ratio (SNR) and the order of a M-ary differential phase-shift keying (M-DPSK) modulation. Such modulation is employed because it can be implemented with non-coherent receivers, thus not requiring phase synchronization between the receiver and the transmitter. This characteristic makes this modulation well-suited for underwater communications. The results show that, for longer transmission ranges, lower modulation orders are optimal from the energy consumption point of view, since the power amplifier dominates the total energy consumption in this scenario. On the other hand, for shorter distances, it makes sense to increase the modulation order, reducing the transmission time in order to minimize the overall energy consumption.

Furthermore, transmission over large distances is typically inefficient in underwater acoustic scenarios, since it often implies in very high transmission power (SOUZA et al., 2016a). Moreover, high transmission power also generates a large amount of interference to the adjacent nodes, considerably reducing the network performance. Therefore, performing multiple hops to transmit information is a viable alternative to the usual single-hop transmission. With multi-hop communication, information frames are sent from source to destination through the collaboration of intermediate relay nodes. Then, despite the new challenges related to delay, routing, and other issues, multi-hop transmissions may help to minimize the total energy consumption. For instance, the authors in (SOUZA et al., 2016a) analyzed how much energy is required to successfully transmit over a multi-hop UWAN. Moreover, the authors compare some of the obtained results with those of a terrestrial wireless communications. The results show that the optimal number of hops for terrestrial wireless communications may be substantially different from that for underwater communications, showing that the proper optimization to the underwater environment can bring important energy savings.

Another approach found in the literature, initially developed by (LIVA et al., 2010) to deliver information in multicast networks, is the use of fountain codes. The main idea of the fountain encoder is to produce an undetermined number of redundant coded packets, where the feedback channel informs when the transmission is completed. Thus, unlike a traditional error correcting codes, fountain codes do not have a fixed code

rate, but they are rather designed to ensure a given target frame error rate (FER) at the receiver without the need of feedback for each transmitted packet. Moreover, another advantage of using the fountain encoder is that it is possible to use simpler error correcting codes in order to obtain the same target performance, thus reducing complexity and energy consumption at both transmitter and receiver. In radio-frequency (RF) wireless networks, fountain codes are a promising solution to decrease collisions and reduce the FER (AOUAMI et al., 2017). However, in (CHEN et al., 2013) it was found out that in 802.11a/g WLANs the cross-layer approach of a higher-layer fountain coding with a PHY layer modulation and forward error correction (FEC) coding in the RF scenario can yield very limited gains.

In the context of UWANs, we have shown in (SIMAO et al., 2016) that the use of fountain codes have been able to reduce up to 30% of the total energy consumption, especially in long-range scenarios, when compared to the case without fountain codes. Moreover, to improve the use of fountain codes in UWANs, the authors in (AHMED, 2017) have proposed two optimization constraints: 1) the transmission power should not exceed a maximum level; and 2) the number of coded packets should not exceed a maximum value dictated by the desired throughput and delay. The fountain codes were compared with a standard automatic repeat request (ARQ) protocol for underwater communications, with results showing that it is possible to achieve relevant energy savings and improvements in terms of throughput efficiency due to the adaptation of transmit power and data rate.

Furthermore, (BARRETO et al., 2017a) proposed a method to reduce the total energy consumption in UWANs by combining fountain codes with BCH error correcting codes. Then, the fountain codes' success rate, the SNR and the BCH code rate were jointly optimized, allowing to increase the link distance with the cost of a gentle degradation in terms of energy efficiency. In addition, a cross-layer FEC scheme using fountain codes in the packet level FEC and channel codes in the bit-level FEC, together with a discrete stochastic approximation (DSA) algorithm to optimize the transmission throughput, is proposed in (CHEN et al., 2018) to improve the reliability of underwater acoustic transmissions. It was found out that the proposed approach brings a performance improvement when compared to other cross-layer strategies. In (LIANG et al., 2018), a transmission redundancy optimization strategy for fountain codes is proposed. The proposed strategy was evaluated against the discrete stochastic approximation (DSA) and the joint power and rate control (JPR) schemes, and it was found out that the proposed structure reduces the transmission redundancy. In addition, the use of fountain codes in order to increase the lifetime of UWANs was also investigated by (YILDIZ, 2019). The

proposed scheme uses a integer linear programming framework in order to minimize the energy consumption. As a result, the use of fountain codes were shown to significantly increase the network lifetime.

The authors in (MOHAMMADI et al., 2020) presented a solution to increase the lifetime of an underwater network using a relay node. However, to maximize the network lifetime it is also necessary to minimize the consumption of the relay node, resulting in the need for multiobjective optimization. To transform the above objectives into a single objective, the weighted sum method is applied, which uses weights, where a convex difference algorithm (DCA) is developed to calculate the optimal solution. In (SIGNORI et al., 2020) the authors relate energy savings to security in underwater communications. Security in UWAN is a little discussed subject, but it makes sense when it comes to risks against military networks and environmental monitoring, where mistakes can have great consequences. In this sense, the authors developed strategies to protect themselves from possible attackers, such as increasing the probability of success packages for faster communication and less consumption.

In (SONG, 2021) an analytical framework for evaluating communication performances of 3D UWAN is presented. In this model, each underwater sensor sends data to its corresponding data sink through Fountain codes-based ARQ transmissions. Furthermore, quality of service (QoS) requirements were implemented, being able to contribute to the extension of IoT, with regard to the ocean, which can be called IoUT. The authors proposed a recursive algorithm to jointly optimize the density of data collectors and the amount of redundancy for fountain codes. The results show that the proposed algorithm works as well as linear search algorithm while significantly decreasing the computing complexity.

In this thesis, we analyze the energy consumption in a multi-hop acoustic underwater network. Moreover, we also assume a feedback channel, so that each hop can retransmit up to a certain number of rounds. The idea is to combine fountain codes with ARQ schemes in order to exploit their complimentary characteristics. For instance, the use of the feedback channel by means of the HARQ scheme may allow the fountain code to adjust the amount of encoded packets, making less use of the channel, reducing the energy consumption. In addition, we also employ a strategy, inspired by (AHMED, 2017), in order to optimize the number of packets used by the fountain codes. However, unlike (AHMED, 2017; BARRETO et al., 2017b; YILDIZ, 2019) our work also considers the impact of the optimization of the modulation order of the M-

DPSK modulation and the SNR in order to minimize the energy consumption. Moreover, we introduce a theoretical analysis, assuming uncoded transmissions, which allows us to derive closed-form expressions for the optimal modulation order, optimal number of hops and optimal number of maximum retransmission attempts per hop. Then, the theoretical analysis is validated against simulations employing punctured convolutional codes, showing good performance agreement. The proposed optimization extends previous results from (SIMAO et al., 2016), which solely considered a single-hop scenario and did not provide any theoretical analysis. Unlike (YILDIZ, 2019), we consider a multi-hop scenario and the M-DPSK modulation, while optimizing these parameters. Our results show that, by optimizing all parameters jointly and by using fountain codes, we can obtain important energy savings, especially for long distances.

Furthermore, unlike (SONG, 2021), which also uses fountain codes and considers only the BPSK modulation and fixed frequency of 200 kHz, our work optimizes the modulation order for $M = 2,4,8$ and 16 and a lower frequency range, factors that could bring different conclusions due to the great attenuation provided by the high frequency.

Moreover, taking into account the conclusions of (CHEN et al., 2013) and the ones presented in our work, it would be erroneous to directly extrapolate the conclusion obtained in the terrestrial scenario to the underwater one. This is because the conclusion obtained in the underwater scenario is the opposite of the one obtained in the terrestrial one: optimized fountain coded bring an energy consumption advantage in underwater acoustic communication systems.

1.1 GOALS

1.1.1 General Goals

The general goal of this document is to analyze the energy consumption in a multi-hop acoustic transmission system employing fountain codes, as well as to provide an optimization algorithm in order to adjust the optimal modulation order, the optimal number of hops and the optimal number of maximum retransmission attempts per hop.

1.1.2 Specific Goals

The developed work has the following specific goals:

- To model the underwater communication channel;
- Investigate the use of fountain codes in the developed model;
- Optimize the number of hops;
- Optimize the number of transmission trials per hop;
- Optimize the M-DPSK modulation order;
- Optimize the number of packets encoded by the fountain code;
- Simulate the performance of this model assuming a convolutional encoder;
- Compare simulation results against a simplified uncoded theoretical model, where the comparison between two commercial modems (WHOI and Evo) are also considered, in order to obtain insights into the system optimization.

1.2 ORGANIZATION OF THE THESIS

The organization of this thesis is as follows. Chapter 2 introduces the underwater acoustic channel, mathematically detailing the characteristics of the attenuation, noise, SNR, fading and error probability. Moreover, we consider the case of the fountain codes and retransmissions, and show how our work is distinguished from the literature.

Chapter 3 provides a description on the proposed optimization, where we optimize the system parameters in order to meet a given target FER. The process of optimizing the number of fountain packets is presented in Algorithm 1, where the main goal is the minimization of the number of fountain packets, while maintaining a valid SNR for transmission. Then, the energy consumption model is presented, where the fountain codes, retransmissions and multiple-hops are considered. Finally, we detail and discuss the individual optimization of the number of hops, retransmissions and modulation order.

In Chapter 4 we present and discuss the numerical results, where the theoretical analysis, which is performed assuming uncoded transmission in Rayleigh fading, is validated against simulations employing conventional convolutional codes, assuming K-fading. Initially, we consider the parameters of the WHOI Modem (FREITAG et al., 2005), but we also further compared it with Evo Modem (EVOLOGICS, 2018). We show several comparisons with variation of parameters, where it is possible to observe the most relevant parameters to be optimized and in which distance ranges the proposed solution

is more efficient. Part of the results obtained were published in (SIMAO et al., 2020). Finally, Chapter 5 gives a summary of this thesis as well as a discussion on directions for future works.

2 UNDERWATER ACOUSTIC CHANNEL CHARACTERISTICS

Sensor networks are revolutionizing many areas of science, industry, and government (HEIDEMANN et al., 2006). The possibility to have small devices physically distributed allows the exploration of the most diverse environments and brings new opportunities, for example with micro-habitat monitoring, structural monitoring, and industrial applications. However, the topology of these networks must take into account the energy consumption, as it can result in a high financial cost, considering that the number of sensors can be high.

Figure 1 – Typical Underwater Network Topology.

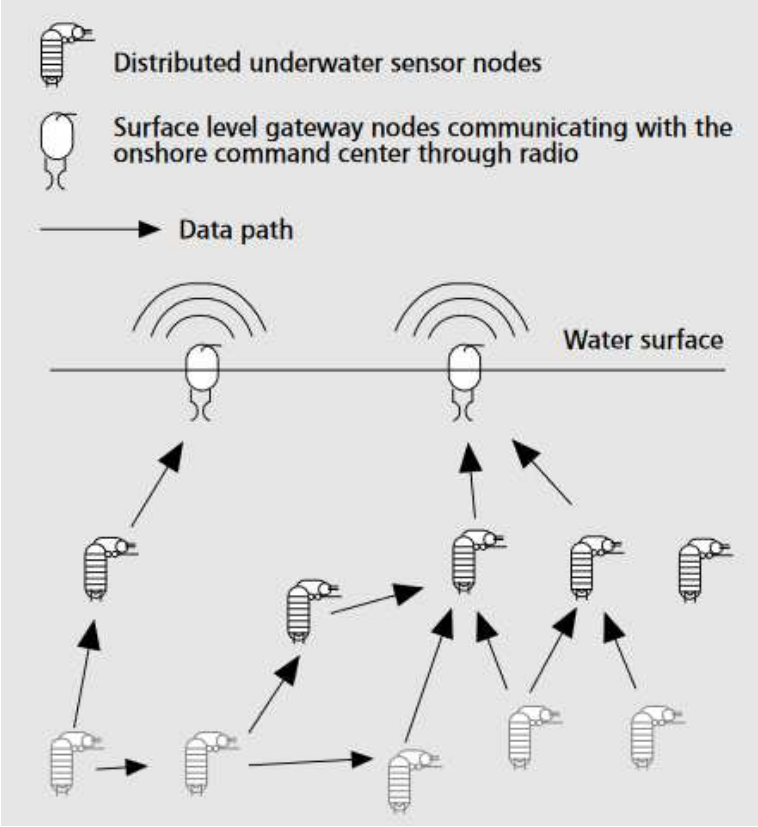

Source: Adapted from (ZHOU, 2006).

Figure 1 illustrates a example of underwater network topology. In this type of network, sensor nodes are deployed to cover a spatial monitoring area. Then, data is collected by local sensors and relayed by intermediate sensors by acoustic signals, and then finally it will reach the surface nodes, which can transmit data to the on-shore command center using RF signals. Considering that this type of network is designed for monitoring over long periods, energy savings are one of the main focuses in the development of

communication protocols (ZHOU, 2006).

The work in (SOUZA et al., 2015) highlights the importance of energy savings in underwater networks, since a large amount of energy is spent to transmit acoustic waves; the authors concluded that the optimization of code rate is vital for a greater energy efficiency, compared to the use of a fixed code rate with convolutional codes, which are popular in commercial devices. For shorter communication distances, the authors in (SOUZA et al., 2015) concluded that a transmission without error correcting codes may be more energy efficient. In order to achieve these conclusions, the authors modeled the code consumption, attenuation and noise, as well as optimized frequency and code rate.

In this work, we consider underwater acoustic transmission in a multi-hop scenario, illustrated by Figure 2. Due to the long distance l between the source node and the gateway, $(\varphi - 1)$ intermediate nodes are employed, so that φ represents the number of hops. We assume that the intermediate nodes are positioned between the source and the destination, with l_k representing k-the hop-distance, as in (1).

$$\sum_{k=1}^{\varphi} l_k = l. \tag{1}$$

Moreover, we also assume that a maximum of τ transmission attempts are allowed at each hop. The communication channel is subjected to attenuation, noise and fading, as will be detailed in the following subsections. Since the channel in the underwater environment is time varying and the data rate in this work is low, we consider a fast fading scenario, where consecutive transmissions are independent and identically distributed.

Figure 2 – System model.

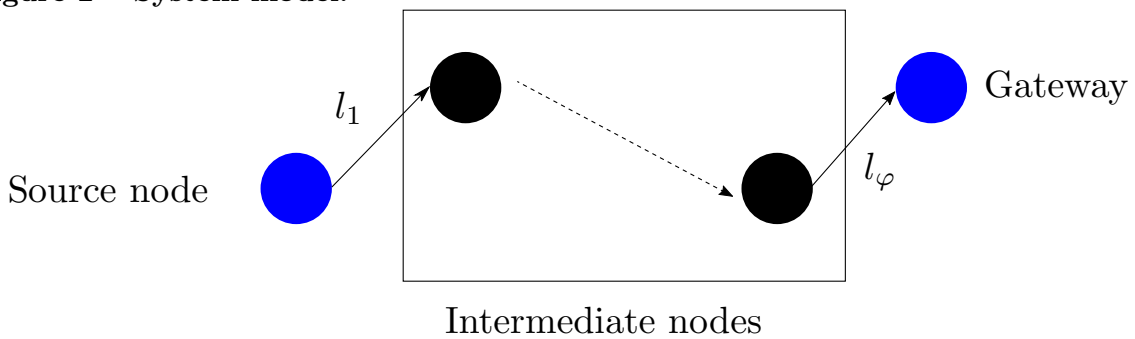

Source: The author.

2.1 ATTENUATION

The path loss in the underwater acoustic communications, usually denoted by absorption loss, is a function of both distance and frequency, thus limiting the available bandwidth. Then, for each k-th hop of Figure 2, the attenuation $A(l_k, f)$, in dB, is given by (STOJANOVIC, 2006)

$$A_{dB}(l_k, f) = 10\kappa \log_{10} l_k + \frac{l_k}{100} \log_{10} a(f), \tag{2}$$

where $A_{dB}(l_k, f)$ is $10\log_{10}\frac{A(l_k,f)}{A_0}$, A_0 is a unit-normalizing constant, $10\kappa\log_{10} l_k$ is the spreading loss, with l_k being expressed in meters, and κ is the propagation geometry. In addition, the absorption loss is represented by $\frac{l_k}{100}\log_{10} a(f)$, with f being the frequency in kHz and $a(f)$ being the absorption coefficient, expressed in dB/km according to (STOJANOVIC, 2006)

$$A_{dB}(f) = \frac{0.11f^2}{1+f^2} + \frac{44f^2}{4100+f^2} + 2.75\cdot 10^{-4} f^2 + 0.003. \tag{3}$$

Figure 3 – Absorption coefficient as a function of the frequency.

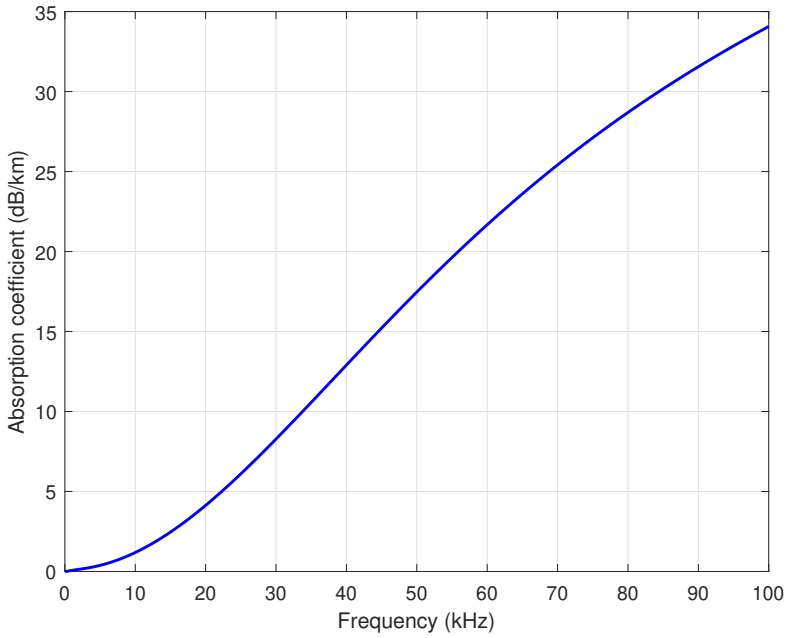

Source: Adapted from (STOJANOVIC, 2006).

Figure 3 shows the absorption coefficient. As we can observe, it increases rapidly with frequency and is the main factor that limits the maximum usable frequency of an acoustic link of a certain distance.

2.2 NOISE

The noise in underwater acoustic environments is characterized by the sounds of the underwater environment that can interfere in the communication. Following (STOJANOVIC, 2006), the underwater noise can be modeled using four sources: turbulence (N_{t}), shipping (N_{s}), waves (N_{w}), and thermal noise (N_{th}), which is the dominant noise. The following empirical formulae give the power spectral density (PSD) of the four noise components:

$$\begin{aligned}
&10\log N_{\mathrm{t}}(f)a = 17 - 30\log_{10} f,\\
&10\log N_{\mathrm{s}}(f) = 40 + 20(s - 0,5) + 26\log_{10} f - 60\log_{10}(f + 0.03),\\
&10\log N_{\mathrm{w}}(f) = 50 + 7.5\sqrt{w} + 20\log_{10} f - 40\log_{10}(f + 0.4),\\
&10\log N_{\mathrm{th}}(f) = -15 + 20\log_{10} f,
\end{aligned} \tag{4}$$

where s is the shipping activity factors, whose value ranges between 0 and 1 for low and high activity, respectively, and w is the wind speed in m/s. Furthermore, let us remark that, as depicted in (STOJANOVIC, 2006), turbulence noise influences only the very low frequency region, below 10 Hz. Noise caused by distant shipping is dominant in the frequency region between 10 Hz and 100 Hz. Surface motion caused by wind-driven waves is the major factor contributing to the noise in the frequency region between 100 Hz and 100 kHz. Finally, thermal noise becomes dominant only when $f > 100$ kHz.

Then, the total noise $N(f)$ is given by adding the four noise components as a following:

$$N(f) = N_{\mathrm{t}}(f) + N_{\mathrm{s}}(f) + N_{\mathrm{w}}(f) + N_{\mathrm{th}}(f). \tag{5}$$

However, to model the noise, we follow the model also proposed in (STOJANOVIC, 2006) in order to approximate this PSD as a function of the frequency, so that

$$10\log_{10} N(f) \approx N_1 - \eta\log_{10} f, \tag{6}$$

where $N_1 = 50$ dB re μPa and $\eta = 18$ dB/decade.

Figure 4 shows the overall PSD of the ambient noise, using 5, and the approximate noise model, using (6). In both cases the noise decays with frequency, thus limiting the useful acoustic bandwidth from below. Moreover, as we can observe, the approximate equation is useful up to a frequency of 10 kHz and much simpler to manipulate mathematically. Thus, the approximate equation is used in this work.

Figure 4 – Overall PSD of the ambient noise and the approximate equation noise, both as function of the frequency.

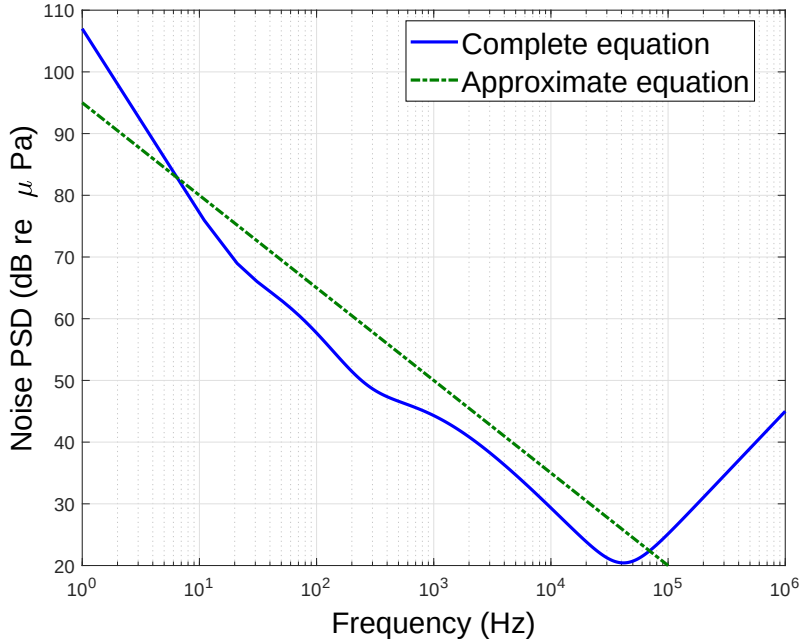

Source: Adapted from (STOJANOVIC, 2006).

2.3 SIGNAL-TO-NOISE RATIO (SNR)

Combining the attenuation $A(l_k, f)$ and the noise PSD $N(f)$ we can write the average SNR as

$$\overline{\gamma}_k(l_k, f) = \frac{\mathcal{P}_{\mathrm{t}}(l_k, f)}{A(l_k, f)\, N(f) M_l B}, \tag{7}$$

where $\mathcal{P}_{\mathrm{t}}(l_k, f)$ is the acoustic transmit power, M_l is the link margin and B is the bandwidth. Finally, the instantaneous SNR can be written as $\gamma_k(l_k, f) = |h|^2\ \overline{\gamma}_k(l_k, f)$, where h denotes the acoustic channel fading.

The factor $(A(l_k, f)N(f))^{-1}$ is illustrated in Figure 5, which is usually denoted as AN product and determines the part of the SNR that depends on the frequency. As we can observe, for each transmission distance l_k, there clearly exists an optimal frequency $f_o(l_k)$ for which the maximal narrow-band SNR is obtained. The optimal frequency $f_o(l_k)$ is illustrated in Figure 6 as a function of the link distance. In practice, one may choose some transmission bandwidth around $f_o(l_k)$, and adjust the transmission power so as to achieve the desired SNR.

Figure 5 – Inverse of the product $A(l_k, f)N(f)$ as a function of the link distance.

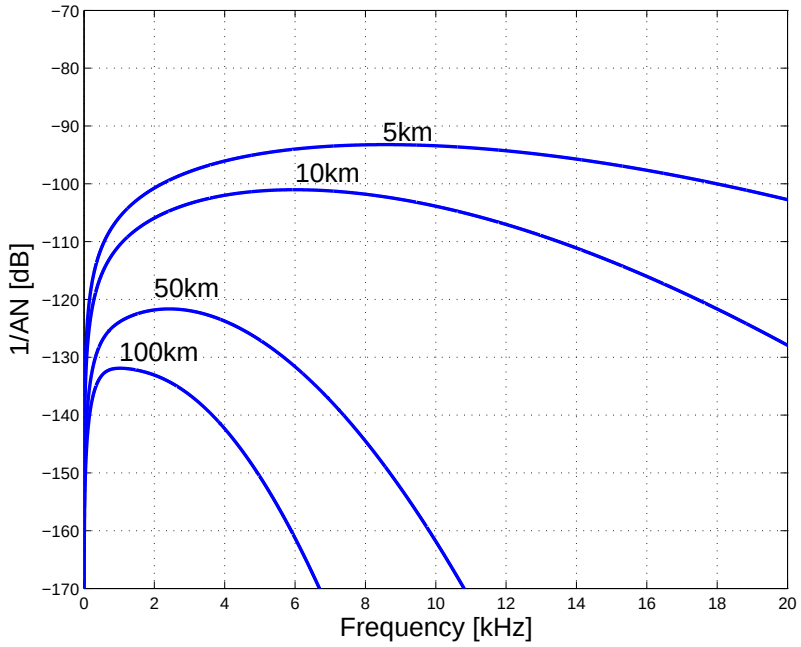

Source: Adapted from (STOJANOVIC, 2006).

2.4 FADING

To model the fading effects, the Rayleigh and Rice distributions are normally used in RF wireless communication. In this thesis we employ both Rayleigh and the K distribution. The K distribution has been chosen since the experimental results in (YANG; YANG, 2006) show a good fit for the underwater scenario. Thus, our simulation results will be carried out using the K distribution in conjunction with convolutional encoding, in order to give a more realistic view of UWANs. On the other hand, since the K distribution provides cumbersome expressions, which is mathematically difficult to handle, our theoretical results employ uncoded Rayleigh fading, aiming to find smaller expressions that will give some insights into the system optimization.

The probability density function of the K distribution is given by the following equation (YANG; YANG, 2006):

$$f_X(x) = \frac{4}{\sqrt{\psi}\Gamma(\nu)} \left(\frac{x}{\sqrt{\psi}}\right)^{\nu} K_{\nu-1}\left(\frac{2x}{\sqrt{\psi}}\right), \tag{8}$$

where ν is a shape parameter, ψ is a scale parameter, $K_{\nu-1}$ is the modified Bessel function of the second kind, of order $\nu - 1$, and $\Gamma(\nu)$ is the Gamma function (GRADSHTEIN et

Figure 6 – Optimal frequency as function of the link distance.

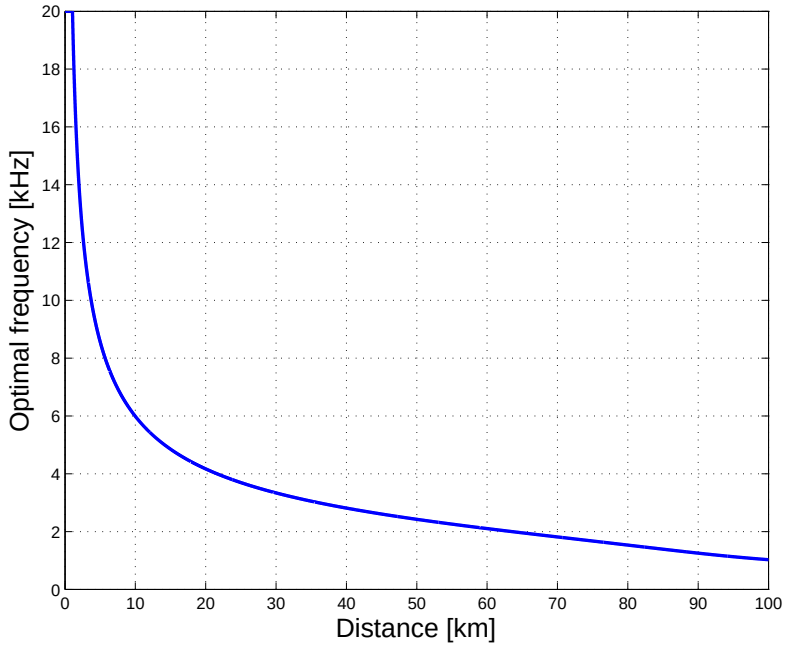

Source: Adapted from (STOJANOVIC, 2006).

al., 2000). Figure 7 shows that when the shape parameter ν is large (about $\nu = 20$), the BER from a system transmitting through a K-distributed channel becomes very close to the one from Rayleigh fading. However, measurements reported in (YANG; YANG, 2006) show that $\nu = 1.5$ may be a good approximation to the fading in an underwater acoustic environment with a frequency range from 15 to 19 kHz [1]; with this configuration K-fading is more severe than Rayleigh. In this sense, a lower ν value indicates a more severe scenario.

2.5 ERROR PROBABILITY

In order to provide a tractable theoretical analysis, we consider an approximation for the BER, $P_b(\overline{\gamma}_k)$, of the M-DPSK modulation considering a Rayleigh distribution for the channel fading, which using (PROAKIS; SALEHI, 2001, eq. (10.4-42)) yields

$$P_{\mathrm{b}}(\overline{\gamma}_k) \approx \frac{M-1}{2M\overline{\gamma}\left[\sin\left(\frac{\pi}{M}\right)\log_2 M\right]^2}, \tag{9}$$

[1] In the numerical results we consider f=10 kHz as in WHOI Modem (FREITAG et al., 2005) with the approximation of $\nu = 1.5$ as in (YANG; YANG, 2006)

Figure 7 – BER comparison between Rayleigh and K distribution.

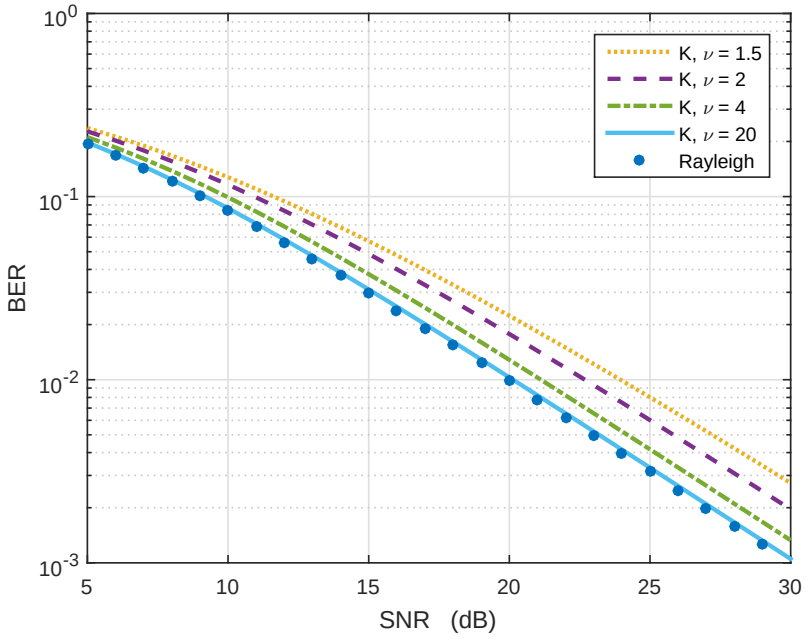

Source: Adapted from (YANG; YANG, 2006).

where we omit the dependence of $\overline{\gamma}$ with (l_k, f) in order to simplify the notation. Moreover, assuming an uncoded payload of L bits, the corresponding frame error rate (FER), $P_{\mathrm{f}}(\overline{\gamma})$, is given by

$$P_{\mathrm{f}}(\overline{\gamma}_k) = 1 - \left[1 - P_{\mathrm{b}}(\overline{\gamma}_k)\right]^L. \tag{10}$$

2.6 FOUNTAIN CODES AND RETRANSMISSIONS

In order to improve reliability, we assume the use of fountain codes (LIVA et al., 2010), whose goal is to encode a group of Z frames into $Y \geq Z$ frames, sent at once over the acoustic link. Then, the probability of success, $P_s(\overline{\gamma}_k)$, becomes a function of the FER in (10) and of the number of packets Y that are used, which can be written as (RAMEEZ; STOJANOVIC, 2013)

$$P_{\mathrm{s}}(\overline{\gamma}_k) = \sum_{z=Z}^{Y} \binom{Y}{z} \left[1 - P_{\mathrm{f}}(\overline{\gamma}_k)\right]^z P_{\mathrm{f}}(\overline{\gamma}_k)^{Y-z}. \tag{11}$$

Furthermore, we complement the use of fountain codes by employing retransmissions at each hop. In this work, a retransmission is characterized when the transmitter, based on the negative feedback information, retransmits the fountain packets. Therefore, each retransmission carries only the fraction of $(1 - P_{\mathrm{f}}^{\star})$ packets that were not

correctly decoded by the receiver, where $P_{\mathrm{f}}^{\star}$ is the target FER. Due to the long delays in communications using underwater acoustic waves, it is important to limit the number of retransmissions. Thus, assuming τ transmission trials, the corresponding FER at each k-th hop is given by

$$P_{\mathrm{f},k}(\overline{\gamma}_k, \tau) = \Big[1 - P_{\mathrm{s}}(\overline{\gamma}_k)\Big]^{\tau}. \tag{12}$$

Finally, after the φ hops between source and destination, the overall FER can be written as

$$P_{\mathrm{f}}(\overline{\gamma}_k, \tau, \varphi) = 1 - \prod_{k=1}^{\varphi} \Big[1 - P_{\mathrm{f},k}(\overline{\gamma}_k, \tau)\Big]. \tag{13}$$

After presenting the relationship between fountain codes and retransmissions and their respective influences on the overall FER, the next chapter will present the optimization of each of these parameters.

3 PROPOSED OPTIMIZATION

In this chapter the optimization of the number of fountain packets, modulation order, number of transmission trials and number of hops are presented in detail.

We optimize the system parameters in order to meet a given target FER $P_{\mathrm{f}}(\overline{\gamma}, \tau, \varphi) = P_{\mathrm{f}}^{\star}$. In (11) we can observe that the probability of successful decoding P_{s} is a function of both FER and number of fountain encoded packets, Y. In other words, for every value of Y (starting with $Y = Z, Z+1, Z+2, \cdots$) there is a corresponding value of $P_{\mathrm{f}}^{\star}(\overline{\gamma}_k)$ for a given P_{s}. However, due to the binomial in (11), the optimization process is mathematically complex. Inspired by the approach proposed in (AHMED, 2017), we present a procedure in order to approximate P_{s} as a function of the FER. This procedure has as its goal the minimization of the number of fountain packets Y, while maintaining a valid SNR for transmission. In order to facilitate the understanding of the procedure, Algorithm 1 summarizes the optimization process. First, we calculate the probability of successful decoding of every Y, from a minimum number of packets $Y_{\min}$ to a maximum number of packets $Y_{\max}$. Then, we set P_{s} equal to the target FER, i.e., $P_{\mathrm{s}} = P_{\mathrm{f}}^{\star}$, and then we use (11) in order to find $P_{\mathrm{f}}(\overline{\gamma}_k)$. Next, we calculate the maximum BER using (10), and we use it to find the corresponding SNR, denoted by $\bar{\gamma}_k(i)$. Finally, we verify if obtaining this SNR at the receiver does not violate the given maximum transmitted power, taking into account the attenuation and the noise. The smallest value of Y where this condition is met is the optimum number of fountain packets Y_{opt}, which will minimize the energy consumption for a given target FER. Values of Y with invalid SNRs are not considered in the optimization process.

As a consequence, the joint numerical optimization carried out through Algorithm 1 process provides an optimal number of coded packets Y_{opt}, which allow us to express (11) as

$$P_{\mathrm{s}}(\overline{\gamma}_k) \approx \beta(Y_{\mathrm{opt}}, \overline{\gamma}_k)\, P_{\mathrm{f}}(\overline{\gamma}_k), \tag{14}$$

where we use $\beta(Y_{\mathrm{opt}}, \overline{\gamma}_k)$ to denote the result of the optimization process, which gives $P_{\mathrm{s}}(\overline{\gamma}_k)$ as a function of $P_{\mathrm{f}}(\overline{\gamma}_k)$, as illustrated by Figure 8.

In order to provide an approximated theoretical analysis, we assume that the intermediate nodes in the network are equally spaced, so that $l_k = \frac{l}{\varphi}$ and $\overline{\gamma}_k = \overline{\gamma}$, $\forall k$. In this case, (13) simplifies to

$$P_{\mathrm{f}}(\overline{\gamma}, \tau, \varphi) = 1 - \left[1 - P_{\mathrm{f},k}(\overline{\gamma}, \tau)\right]^{\varphi}. \tag{15}$$

Algorithm 1 Optimization Process

Input: $P_{\mathrm{f}}^{\star}$, $Y_{\min}$, $Y_{\max}$, $A(l_k, f)$, $N(f)$, $\mathcal{P}_{\mathrm{t}}$;
$\bar{\gamma}_k = \infty$
$Y_{\mathrm{opt}} = \infty$
for $i = Y_{\min}$ to $Y_{\max}$ **do**
    compute $P_{\mathrm{f}}(i)$ in (11) corresponding to $P_{\mathrm{s}}(i) = P_{\mathrm{f}}^{\star}$
    compute $P_{\mathrm{b}}(i)$ using (10)
    compute the corresponding SNR $\bar{\gamma}_k(i)$ using (9)
    if $\bar{\gamma}_k(i) A(l_k, f) N(f) > \mathcal{P}_{\mathrm{t}}$ **then**
        i is invalid
    else
        $Y_{\mathrm{opt}} = \min\{i, Y_{\mathrm{opt}}\}$
    end if

    end for
    Output: $\beta(Y_{\mathrm{opt}}, \bar{\gamma}(i))$

Figure 8 – Probability of successful decoding (P_{s}) as a function of the FER (P_{f}).

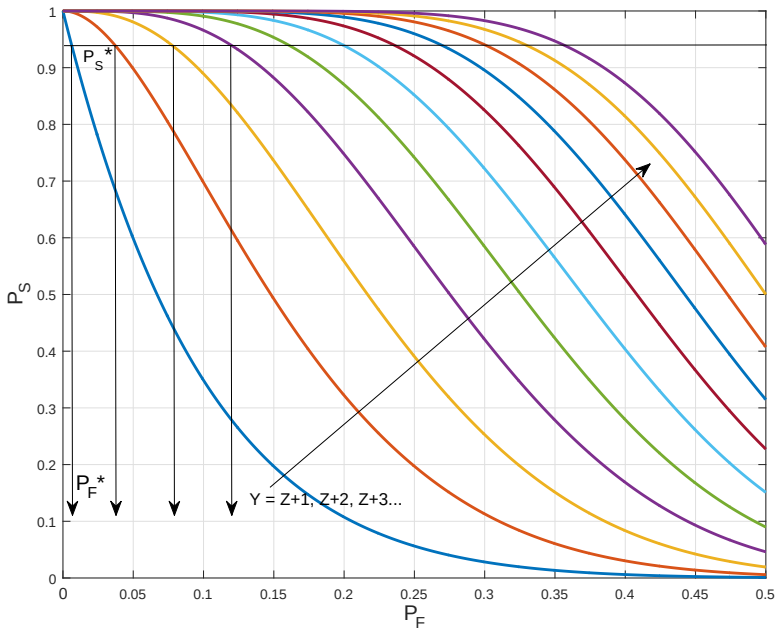

Source: The Author.

Then, combining (9)-(13), replacing (11) by (14), we can write the target BER as

$$P_{\mathrm{b}}^{\star} = 1 - \left\{ \frac{\beta - 1 + \left[1 - (1 - P_{\mathrm{f}}^{\star})^{\frac{1}{\varphi}}\right]^{\frac{1}{\tau}}}{\beta} \right\}^{\frac{1}{L}}, \tag{16}$$

where we drop the dependency of β with Y_{opt} and $\overline{\gamma}$ for simplicity. Furthermore, using

(7) we have that

$$\overline{\gamma}^{\star} = \frac{M-1}{2MP_{\mathrm{b}}^{\star}\left[\sin\left(\frac{\pi}{M}\right)\log_2 M\right]^2}. \tag{17}$$

3.1 ENERGY CONSUMPTION

Considering the use of fountain codes, retransmissions and multiple-hops, the total energy consumption, $\epsilon_{\mathrm{bT}}(\tau,\varphi)$, for each successfully transferred bit can be written as

$$\epsilon_{\mathrm{bT}}(\tau,\varphi) = \frac{\varphi\left[\epsilon_{\mathrm{tx}}(\tau,\varphi)+\epsilon_{\mathrm{rx}}(\tau,\varphi)\right]}{1-P_{\mathrm{f}}^{\star}} \cdot \frac{Y}{Z}, \tag{18}$$

where $\epsilon_{\mathrm{tx}}(\tau,\varphi)$ is the energy consumed by each transmitter for each successfully transferred bit, $\epsilon_{\mathrm{rx}}(\tau,\varphi)$ is the energy spent for transmitting the corresponding feedback bits for acknowledgement and retransmission requests, while $\frac{Y}{Z}$ is the ratio of frames used by the fountain code. Moreover, the term $\frac{1}{1-P_{\mathrm{f}}^{\star}}$ accounts for the additional energy spent with unsuccessful transmitted frames, recalling that $P_{\mathrm{f}}^{\star}$ is the target FER.

Following (SOUZA et al., 2016a), the energy consumed by the transmitter for each successfully transferred bit is

$$\epsilon_{\mathrm{tx}}(\tau,\varphi) = \left[\left(P_{\mathrm{el,tx}}+P_{\mathrm{PA}}\right)T + P_{\mathrm{el,rx}}\,T_{\mathrm{f}}\right]\tau, \tag{19}$$

where $P_{\mathrm{el,tx}}$ is the power consumption of baseband operations and all electronic components for transmitting, $P_{\mathrm{el,rx}}$ is the equivalent for receiving the feedback bits, P_{PA} is the power used by the power amplifier, T is the average transmission time per payload bit per transmission trial, and T_{f} is the feedback time per bit.

Equivalently, at the receiver we have

$$\epsilon_{\mathrm{rx}}(\tau,\varphi) = \left[P_{\mathrm{el,rx}}\,T + \left(P_{\mathrm{el,tx}}+P_{\mathrm{PA}}\right)T_{\mathrm{f}}\right]\tau. \tag{20}$$

The average transmission time per payload bit is a function of the bit rate, R_b, and of the number of bits per symbol. Thus,

$$T = \frac{1}{R_{\mathrm{b}}\log_2 M}. \tag{21}$$

Similarly, the feedback time per payload bit, assuming that only binary modulation is used for the feedback, is given by

$$T_{\mathrm{f}} = \frac{F}{R_{\mathrm{b}}\,L}, \tag{22}$$

where F is the number of feedback bits, where the use of a binary modulation is considered due to high reliability and so we also consider this feedback link error free.

Then, the power consumed by the power amplifier, in Watts, is given by (GAO et al., 2012)

$$\mathcal{P}_{\mathrm{PA}}\left(l_k, f\right) = \mathcal{P}_{\mathrm{t}}\left(l_k, f\right) \frac{10^{-17.2}\ \alpha}{\phi}, \tag{23}$$

where $10^{-17.2}$ is a conversion factor, α is the PAPR of the transmitted signal, which depends on the modulation order, and ϕ is the overall efficiency of the power amplifier and transducer. Moreover, let us recall that $\mathcal{P}_{\mathrm{t}}\left(l_k, f\right)$ is the acoustic transmit power, obtained from (7).

Finally, plugging (17) into (18), we approximate the average total energy consumption by

$$\overline{e}_{\mathrm{bT}} = \frac{Y_{\mathrm{opt}}\varphi\tau(T+T_{\mathrm{f}})}{Z(1-P_{\mathrm{f}}^{\star})}\left(P_{\mathrm{el}} + \frac{\Upsilon(M-1)}{2MP_{\mathrm{b}}^{\star}\left[\sin\left(\frac{\pi}{M}\right)\log_2 M\right]^2}\right), \tag{24}$$

where $P_{\mathrm{el}} = P_{\mathrm{el,tx}} + P_{\mathrm{el,rx}}$ and Υ is given by

$$\Upsilon = A\left(\frac{l}{\varphi}, f\right) N(f)\, M_l\, B\, \frac{10^{-17.2}\ \alpha}{\phi}. \tag{25}$$

3.2 OPTIMAL MODULATION ORDER

In order to find the optimal modulation order, M_{opt}, we first derive (24) with respect to M, yielding

$$\frac{\partial \overline{e}_{\mathrm{bT}}}{\partial M} = \frac{Y_{\mathrm{opt}}\,\varphi\,\tau\left[K_2 + M\left(K_3 + K_4\right)\right]}{Z\,R_{\mathrm{b}}\,P_{\mathrm{b}}^{\star}(1-P_{\mathrm{f}}^{\star})\,K_1} \cdot \csc^2\left(\frac{\pi}{M}\right), \tag{26}$$

where

$$K_1 = \ln(2)\left(M\log_2 M\right)^3, \tag{27}$$

$$K_2 = -(M-1)\,\Upsilon\,\pi\cot\left(\frac{\pi}{M}\right)\left(\ln 2 + R_{\mathrm{b}}T_{\mathrm{f}}\ln M\right), \tag{28}$$

$$K_3 = \frac{\Upsilon}{2}\left\{\frac{3(M-1)}{\log_2 M} + R_{\mathrm{b}}T_{\mathrm{f}}\left[2\left(M-1\right) - \frac{\ln 2}{R_{\mathrm{b}}T_{\mathrm{f}}} - \ln M\right]\right\}, \tag{29}$$

$$K_4 = M\,P_{\mathrm{b}}^{\star}\,P_{\mathrm{el}}\log_2 M \sin^2\left(\frac{\pi}{M}\right). \tag{30}$$

Finally, the optimal modulation order M_{opt} that minimizes the total energy

consumption is obtained by finding M that yields

$$\frac{K_2 + M(K_3 + K_4)}{K_1} \cdot \csc^2\left(\frac{\pi}{M}\right) = 0. \tag{31}$$

Notice that (31) can be easily solved with any numerical method, since it is a function of a single variable, M.

3.3 OPTIMAL NUMBER OF TRANSMISSION TRIALS

We also optimize the number of transmission trials τ. Therefore, we need to derive (24) with respect to τ as follows:

$$\frac{\partial \overline{e}_{\mathrm{bT}}}{\partial \tau} = \frac{Y_{\mathrm{opt}}\,\varphi\,(T + T_{\mathrm{f}})}{Z\left(1 - P_{\mathrm{f}}^{\star}\right)} \left(P_{\mathrm{el}} + \frac{G_3\left[(1-G_2)^L G_2 L\beta + G_1 \ln(G_1)\,(G_2 - 1)\right]}{G_2^2\,(1-G_2)^L}\right), \tag{32}$$

where

$$G_1 = \left[1 - (1 - P_{\mathrm{f}}^{\star})^{\frac{1}{\varphi}}\right]^{\frac{1}{\tau}}, \tag{33}$$

$$G_2 = 1 - \left(\frac{\beta + G_1 - 1}{\beta}\right)^{\frac{1}{L}}, \tag{34}$$

$$G_3 = \frac{(M-1)\Upsilon}{2ML\beta\left[\sin\left(\frac{\pi}{M}\right)\log_2 M\right]^2}. \tag{35}$$

Then, the optimal number of transmission trials τ_{opt} that minimizes the total energy consumption is obtained by finding τ so that

$$P_{\mathrm{el}} + \frac{G_3\left[(1-G_2)^L G_2 L\beta + G_1 \ln(G_1)\,(G_2 - 1)\right]}{G_2^2\,(1-G_2)^L} = 0. \tag{36}$$

3.4 OPTIMAL NUMBER OF HOPS

Finally, we find the optimal number of hops φ_{opt} by doing

$$\frac{\partial \overline{e}_{\mathrm{bT}}}{\partial \varphi} = \frac{Y_{\mathrm{opt}}\,(T + T_{\mathrm{f}})}{Z(1 - P_{\mathrm{f}}^{\star})} \left[P_{\mathrm{el}}\,\tau + \frac{W_1\,(W_2\tau + W_3)}{W_2^2}\right], \tag{37}$$

where

$$W_1 = \frac{(M-1)\,\Upsilon\,\beta^{\frac{1}{L}}}{2M\left[\sin\left(\frac{\pi}{M}\right)\log_2 M\right]^2} \tag{38}$$

$$W_2 = (-1)^{\frac{L+1}{L}}\left\{1-\left[1-(1-P_{\mathrm{f}}^{\star})^{\frac{1}{\varphi}}\right]^{\frac{1}{\tau}}-\beta\right\}^{\frac{1}{L}}+\beta^{\frac{1}{L}}, \tag{39}$$

$$W_3 = \frac{\ln(1-P_{\mathrm{f}}^{\star})}{L\,\varphi}(-1)^{\frac{L+1}{L}}W_1^{1-\tau}\,(1-W_1^{\tau})\,(1-W_1-\beta)^{\frac{1-L}{L}}, \tag{40}$$

so that the optimal number of hops φ_{opt} that minimizes the total energy consumption is obtained by solving the following equation with respect to φ

$$P_{\mathrm{el}}\,\tau+\frac{W_1\,(W_2\tau+W_3)}{W_2^2}=0. \tag{41}$$

4 NUMERICAL RESULTS

In this section we present some numerical results following, as much as possible, the parameters of the WHOI modem (FREITAG et al., 2005), summarized in Table 1. The Micro-Modem WHOI is a compact, low-power, underwater acoustic communications and navigation subsystem. This modem is widely used and operates at a fixed code rate, using a convolutional code (FREITAG et al., 2005). First, we conduct a theoretical analysis assuming uncoded transmissions in Rayleigh fading, which allows us to evaluate all the framework developed in Chapter 3 in terms of optimal modulation order, optimal number of hops and optimal number of maximum retransmission attempts per hop. Next, the theoretical analysis is validated against simulations employing conventional convolutional codes of rate $\frac{2}{3}$ from (BEGIN et al., 1990), assuming a K-fading environment with $\nu = 1.5$.

Table 1 – Simulation Parameters

Parameter	Description	Value
L	Frame payload	64 bytes
B	Bandwidth	320 Hz
F	Feedback frame length	1 bytes
R_{b}	Bit rate	160 bps
$P_{\mathrm{el,rx}}$	Receiver power consumption	1 W
$P_{\mathrm{el,tx}}$	Transmitter power consumption	0 W [1]
$P_{\mathrm{PA,min}}$	Minimum transmit power	8 W
$P_{\mathrm{PA,max}}$	Maximum transmit power	50 W
ϕ	Efficiency of the PA-transducer	0.25
M_l	Link margin	20 dB
f	Frequency	10 kHz
Z	Number of original fountain packets	10
$Y_{\max}$	Maximum number of extra packets	60

Source: (FREITAG et al., 2005)

4.1 THEORETICAL ANALYSIS

The theoretical results will be presented as follows in order to validate the proposed optimizations in Chapter 3.

[1] $P_{\mathrm{el,tx}}$ is considered 0 W, as it is not differentiated from P_{PA} in the WHOI Modem datasheet. Thus, the value of $P_{\mathrm{el,tx}}$ is already being considered in P_{PA}.

4.1.1 Parameter Optimization

In this subsection we present the optimization results for each parameter separately.

Figure 9 – Total energy consumption for different M and the M_{opt} obtained by the numerical solution of (31) as a function of the link distance.

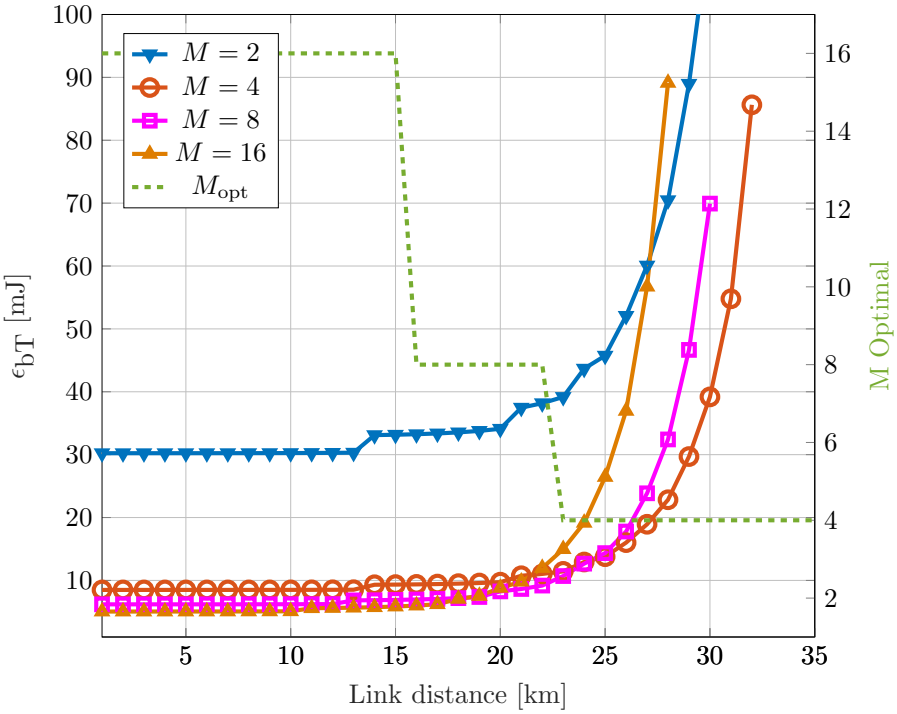

Source: Author.

Figure 9 shows the total energy consumption when employing different modulation orders (with $M \in \{2,4,8,16\}$), obtained by (24), as a function of the link distance. Moreover, we first assume that $\tau = 1$ and $\varphi = 1$. The optimal modulation order, M_{opt}, obtained by the numerical solution of (31) is also shown in the right side of the figure, showing perfect agreement with the obtained results. As we observe, higher modulation orders consume less energy at shorter distances; thus, in this scenario the power amplifier dominates the total energy consumption. Let us remark that, due to the configurations of the WHOI modem, the minimum transmit power is of $P_{\text{PA,min}} = 8$ W. This way, higher modulation orders reduce the transmission time of the packets. On the other hand, when the transmission range increases, the optimal modulation order must be reduced in order to comply with the desired FER that in this case is $P_{\text{f}}^{\star} = 10^{-2}$.

Figure 10 – Total energy consumption for the case with and without retransmission, and the τ_{opt} obtained by the approximate numerical solution of (36) as a function of the link distance.

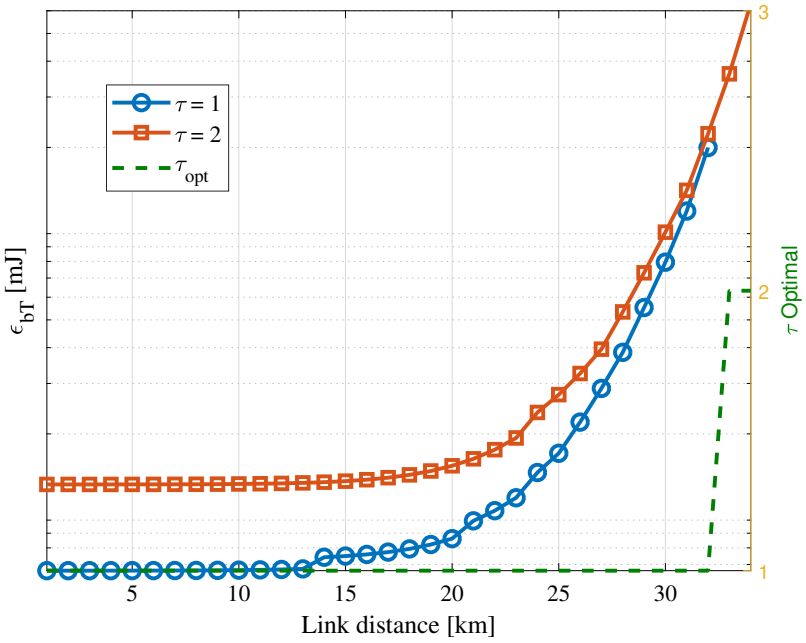

Source: Author.

Figure 10 plots the energy consumption using (24) for the case with and without retransmission in a single-hop scenario ($\varphi = 1$) and with $M = 16$. We limit the transmission trials to $\tau = 2$ due to the fact that this is optimal only in scenarios with a link distance longer than 30 km. In this case, the optimal number of retransmissions was obtained by the numerical solution of (36). As in (SOUZA et al., 2016a), the energy spent by the circuitry is very significant at lower distances, which makes $\tau = 1$ more energy efficient up to a certain total link distance. It is also possible to see that adding the extra retransmission makes sense only in a scenario with very long hops (longer than 30 km). Therefore, retransmissions were not explored much in this work and we used the maximum of $\tau = 2$ in the sequence of this work. This same behavior will be observed in Figure 13, where the retransmissions are not effective using fountain codes, different from the case without fountain codes.

Figure 11 – Total energy consumption for different number of hops (φ) and the φ_{opt} obtained by the numerical solution of (41) as a function of the link distance.

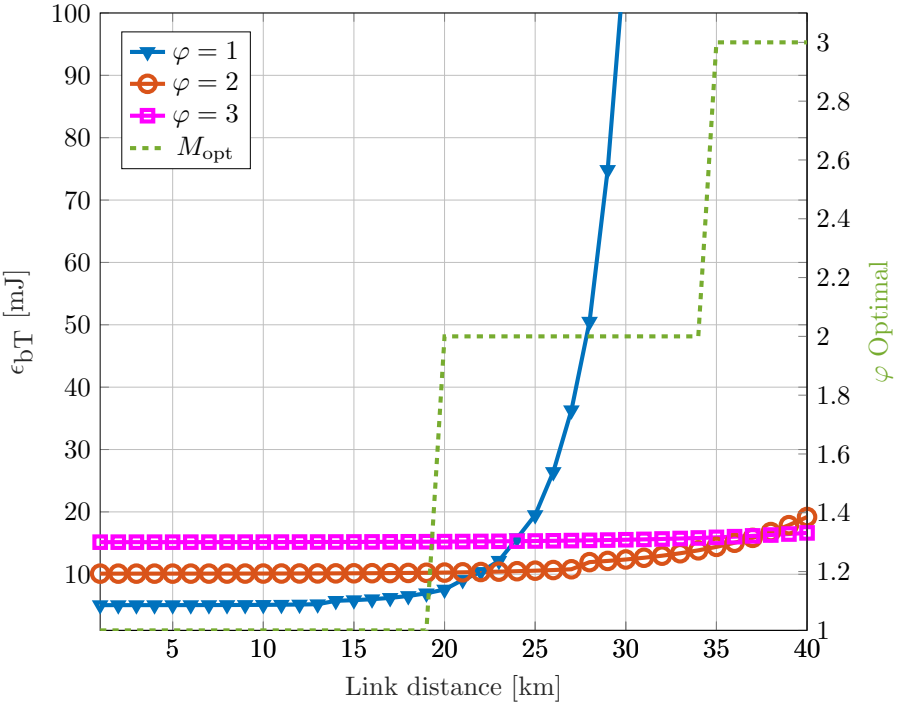

Source: The Author.

Figure 11 plots the energy consumption for different number of hops (φ) when retransmissions are not allowed ($\tau = 1$), also with $M = 16$; the value of φ_{opt} was obtained by the numerical solution of (41). As in τ_{opt}, φ_{opt} depends both on the consumption of electronic circuits and the power amplifier, which depends on the distance of each hop. The results show that $\varphi = 1$ and $\varphi = 2$ are optimal during almost 36 km, indicating that a short number of hops is normally more energy efficient, while $\varphi = 3$ is interesting for long range applications.

4.1.2 Fountain Codes

The following results show comparisons between transmissions with and without fountain codes, including optimizing M, τ and φ.

Figure 12 presents a comparison of the energy consumption when each parameter is individually optimized in a system with or without fountain codes. This evaluation takes into account a maximum acoustic transmit power of 167 dB re μPa. It is possible to see that when using fountain codes for short distances, there is no parameter that stands out in the optimization, but for long distances it is important to optimize the number of hops

in order to obtain the lowest possible energy consumption. On the other hand, when not using fountain codes the most important parameters to optimize are the modulation order and the number of hops. It is also possible to see that the usage of fountain codes brings a significant reduction in energy consumption.

Figure 12 – Energy Consumption for modulation order (M), transmission trials (τ) and number of hops (φ) individually optimized as a function of the link distance.

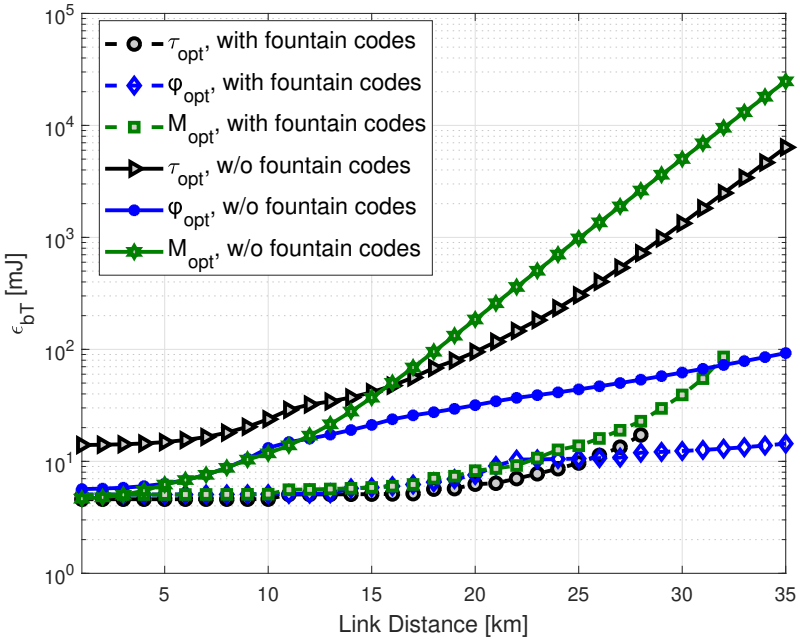

Source: The Author.

Figure 13 (Side A, on the left) shows the main combination of parameters that minimize the energy consumption as a function of link distance in the case without fountain codes. Is possible to see that higher modulation orders are dominant throughout the considered distance range, with different configurations for the number of hops and retransmissions. This shows that the joint optimization of all parameters is essential for maximizing the energy savings. Figure 13 (Side B, on the right) shows the energy consumption when each parameter is individually optimized in a system that uses fountain codes. This evaluation takes into account a maximum transmit power of 167 dB re μPa. It is possible to see that when using fountain codes it is important to optimize the number of hops and the modulation order in order to obtain the lowest possible energy consumption. However, it is worth it to optimize the number of retransmissions only for a long distance scenario, unlike the case without fountain codes, where $\tau = 2$ is optimal for a large distance range.Therefore, we do not focus on retransmissions in this work.

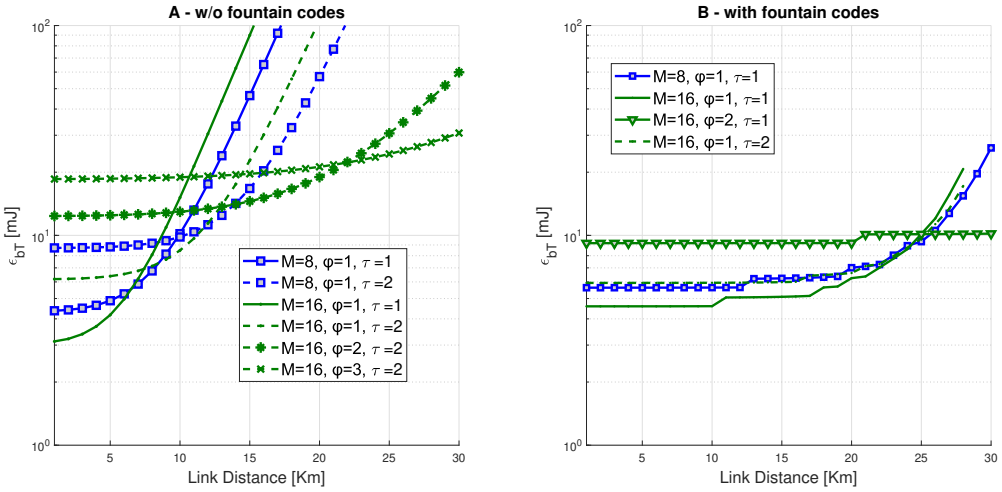

Figure 13 – The best combination of parameters using fountain codes that minimize the energy consumption as a function of link distance.
Source: The Author.

The number of fountain code encoded packets Y for a minimum value of packets $Z = 10$, for different number of hops φ is shown in Figure 14 for $M = 2$ and $\tau = 1$, as a function of the link distance. In addition, we have limited Y to a maximum of $Y_{\max} = 60$ in our simulation setup to avoid excessive congestion of the acoustic link; we also consider a target FER of 10^{-2}. Clearly, we can see that Y considerably increases with the distance. However, when we increase the number of hops, the SNR remains high for longer distances. Thus, Y takes longer to increase and reach saturation, which happens when the power limit is exceeded. In this case, more packets are needed to maintain the target FER. The distance where saturation occurs (i.e., $Y = 60$ is not enough to obtain the target FER) for $M = 2, 4$ and 8 is presented in Table 2 for different numbers of hops. It is seen that transmissions using higher modulation orders $M = \{8, 16\}$ require considerably more packets to successfully reach the target FER, so that the saturation effect is observed rapidly.

Figure 14 – Number of packets encoded by the fountain code Y as a function of the link distance for 2-DPSK.

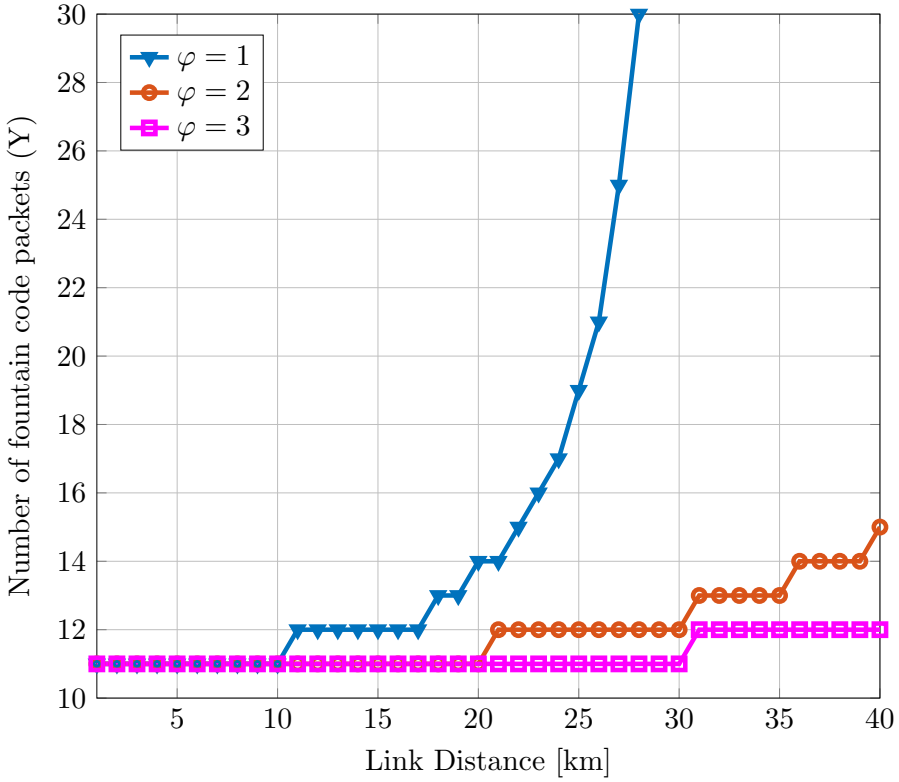

Source: The Author.

Table 2 – Distance for Fountain Packets Saturation in the Uncoded Scheme

Number of Hops	Modulation	Saturation Distance (km)
1	4-DPSK	34
1	8-DPSK	31
1	16-DPSK	27
2	4-DPSK	40
2	8-DPSK	40
2	16-DPSK	40

Source: The Author.

Figure 15 compares the total energy consumption with all parameters being optimized in the cases with and without fountain codes. As it is possible to observe, the energy consumption is similar for very short transmission distances, with a small advantage to the case without fountain codes, making sense not to use coding for short distances (up to 5 km). However, a significant amount of energy can be saved by employing fountain codes throughout the distance range, with up to 37% of energy savings. This reduction in the energy consumption is linked to the fact that fountain codes allow to increase the packet success rate, considerably decreasing the transmit power at the cost

Figure 15 – Total energy consumption comparison as a function of the link distance.

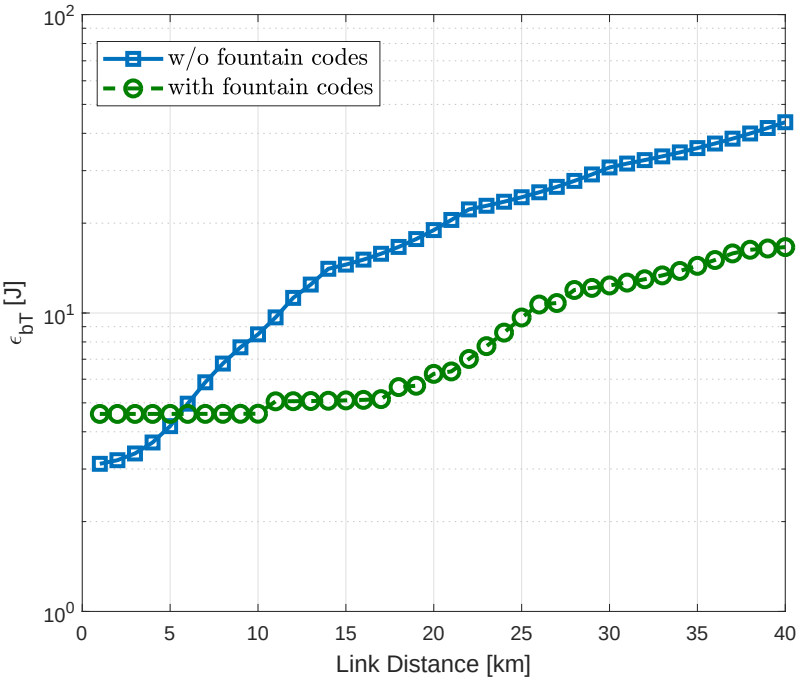

Source: The Author.

of sending extra redundant packets.

4.1.3 Random Node Deployment

Here we present a variation of the results with the nodes spaced randomly, unlike from the rest of the results, where we consider the nodes equally separated.

Figure 16 illustrates a more general scenario, where the intermediate nodes are randomly deployed between the source and the destination, with a total of 10000 trials for an average performance, φ=2 hops, $\tau = 1$ and the target FER is $P_{\mathrm{f}} = 10^{-2}$. Moreover, the modulation order and the number of fountain code packets are optimized to reduce the energy consumption. As we observe in this example, the use of fountain codes is even more important to reduce the energy consumption compared to the scenario where the nodes are equally spaced. This is because, in this scenario, longer links appear more often, so that fountain codes with optimized number of packets become more important.

Figure 16 – Total energy consumption when the intermediate nodes are randomly deployed between the source and the destination, with a total of 10000 trials, φ=2 hops, $\tau = 1$ and the target FER is P_f=10^{-2}.

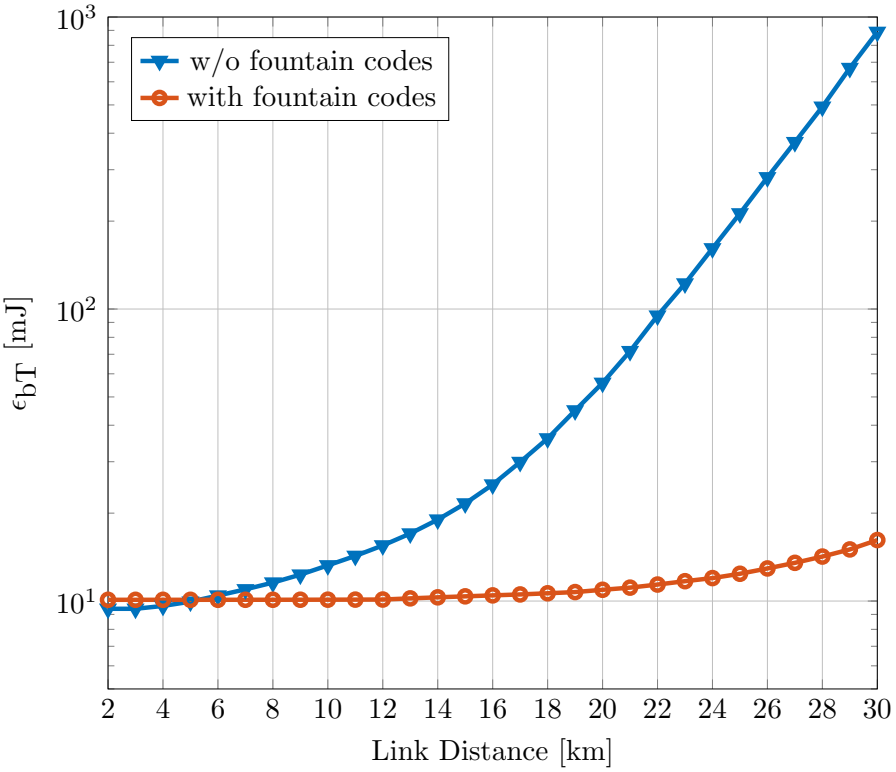

Source: The Author.

4.1.4 WHOI Modem vs. Evo Modem

To verify if the conclusions reached above hold up for different system parameters, we also present a comparison of the results obtained with the parameters inspired by the WHOI modem from (FREITAG et al., 2005) (which are summarized in Table 1) with ones inspired by the EvoLogics S2CR 48/78 modem (which are summarized in Table 3), due to the fact that it is a commercial modem, more modern and because it operates at a high frequency. Unlike WHOI Modem, which is a modem for scientific purposes.

Table 3 – Evo Logics S2CR 48/78 Parameters x WHOI Modem

Parameter	Evo Logics	WHOI Modem
Carrier Frequency	48 kHz	10 kHz
Data Rate	31.2 kbit/s	160 bit/s
Transmitter Power	5.5 W - 60 W	8 W - 50 W
Receiver Power	0.8 W	1 W

Source: The Author.

Figure 17 – Total energy consumption comparison as a function of the link distance for two different modem, with $\tau = 1$.

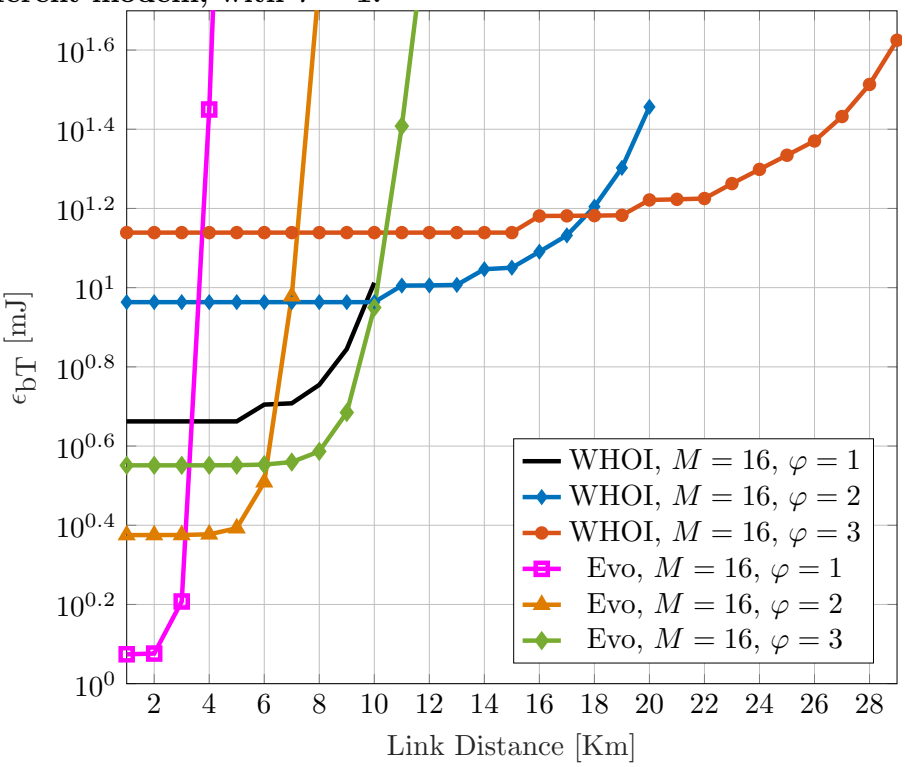

Source: The Author.

In Figure 17 we show the comparison between WHOI Modem and EvoLogics, where is possible to observe that the same behavior (the usage of a high modulation order and an emphasis on using more hops to reduce the energy consumption) is presented for both configurations; however, when using the EvoLogics modem parameters saturation is reached earlier, due to the shorter range of this modem and the highest frequency and maximum power.

4.1.5 Different Target FERs

In this thesis we optimize the system parameters in order to meet a given target FER. Therefore, we now compare the energy consumption for different target FERs.

The energy consumption when using $M = 16$ and $\varphi = 1$ and $\tau = 1$ for different target FERs (from 10^{-1} to 10^{-4}) is presented in Figure 18 the link distance is limited to 25 km due to the saturation of the fountain packets. It can be seen that decreasing the target FER does not lead to a significant increase in energy consumption. Also, the number of fountain packets does not sharply increase with a higher target FER.

Figure 18 – Total energy consumption comparison for different FERs, M=16, φ=1 and τ=1

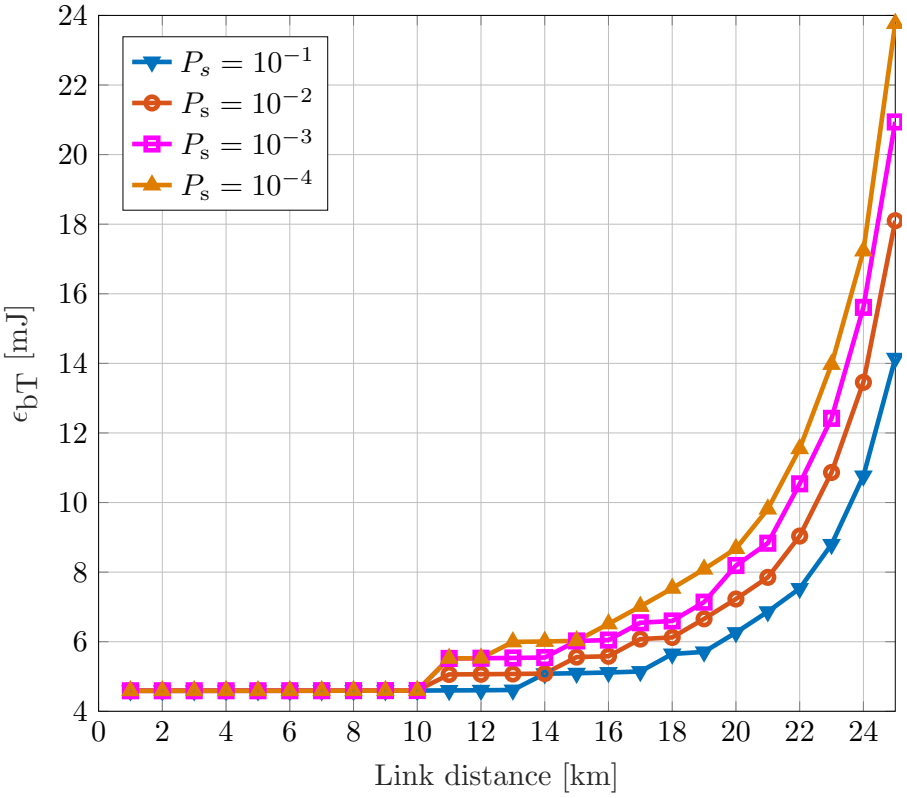

Source: The Author.

4.1.6 Rayleigh vs. K-Fading

In this thesis we employ both Rayleigh and the K-fading. Therefore, it makes sense to compare both in terms of energy consumption.

Figure 19 compares the energy consumption when all parameters are optimized in a system subjected to K-fading and Rayleigh. This evaluation takes into account a maximum acoustic transmit power of 167 dB re μPa and the BER is calculated using the numerical evaluation of (8), assuming $\nu = 1.5$ for the K-fading and $K = 20$ as an approximation for Rayleigh fading. It is possible to see that when using Rayleigh the energy consumption is lower due to the fact that it considers a less severe scenario than K-fading.

Figure 19 – Total energy consumption comparison for *K*-fading and Rayleigh

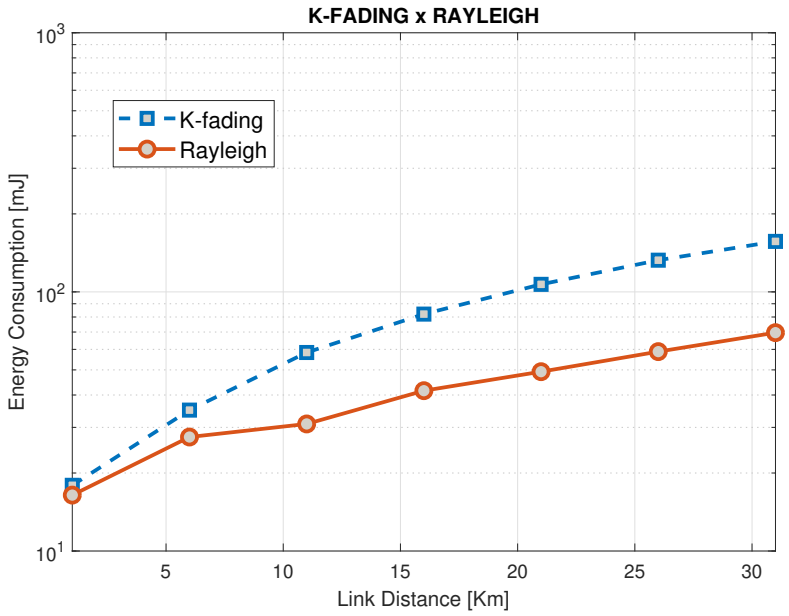

Source: The Author.

4.2 SIMULATION RESULTS EMPLOYING CONVOLUTIONAL CODES

In this section, simulation results are presented. In addition to fountain codes, and inspired by (FREITAG et al., 2005) we consider the optimized conventional convolutional codes of $r = \frac{2}{3}$ from (BEGIN et al., 1990). Thus, we need to consider the additional energy spent to encode at the transmitter, decode at the receiver and the code rate into the total energy consumption $\hat{\epsilon}_{\mathrm{bT}}(\tau, \varphi)$, as follows

$$\hat{\epsilon}_{\mathrm{bT}}(\tau,\varphi) = \frac{\varphi\left[\tau\left(\epsilon_{\mathrm{enc}}+\epsilon_{\mathrm{dec}}\right)+\epsilon_{\mathrm{tx}}(\tau,\varphi)+\epsilon_{\mathrm{rx}}(\tau,\varphi)\right]}{r\left(1-P_{\mathrm{f}}^{\star}\right)}\cdot\frac{Y}{Z}, \tag{42}$$

where ϵ_{enc} is the energy spent to encode each symbol, while ϵ_{dec} is the energy spent to decode, which can be modeled as (ROSAS; OBERLI, 2012)

$$\epsilon_{\mathrm{enc}} = \epsilon_{\mathrm{dec}} = \frac{V_{dd} I_0}{r\, L\, f_{\mathrm{APU}}} \sum_{j=1}^{J} c_j n_j, \tag{43}$$

where J is the number of different types of arithmetic operations required for encoding, c_j is the number of clock cycles required by that operation and n_j is the number of times such operation is performed during the encoding/decoding algorithm. Moreover, V_{dd} is the arithmetic processing unit APU operating voltage, I_0 is the average current during the execution time of the arithmetic operations, and f_{APU} is the APU's clock frequency.

In addition, in coded transmissions, each forward frame carries H header bits with essential transmission parameters, an overhead composed of O bits, and a payload composed by rL bits of data and $(1-r)L$ additional bits for coding. Thus, the average transmission time, $\hat{T}$, per payload bit per transmission trial is modified as follows

$$\hat{T} = \frac{L+H+O}{r\,L\,R_{\mathrm{b}}\log_2 M}. \tag{44}$$

Similarly, the feedback time per payload bit, $\hat{T}_{\mathrm{f}}$, becomes

$$\hat{T}_{\mathrm{f}} = \frac{F}{r\,R_{\mathrm{b}}\,L}. \tag{45}$$

Table 4 lists the employed simulation parameters.

Table 4 – Simulation Parameters for the Convolutional Codes

Parameter	Description	Value
H	Frame Header	2 bytes
O	Overhead	2 bytes
f_{APU}	APU frequency	20 MHz
V_{dd}	APU voltage	3 V
I_0	Average current	6.37 mA
c_j	Number of clock cycles per operation	1 cycle
ν	K-distribution shape parameter	1.5
r	Code rate	$\frac{2}{3}$

Source: The Author.

Figure 20 presents the simulation results that compares the total energy consumption with all parameters being optimized in the cases with fountain codes and convolutional codes, for a fixed code rate $r = 2/3$. As it is possible to observe, the energy consumption is similar for very short transmission distances at up to 6 km. However, a significant amount of energy can be saved by employing fountain codes throughout the distance range, with savings of up to 40%. This result validates the theoretical analysis presented in Figure 15. In addition, Table 5 presents the optimal parameters to minimize the energy consumption for each link distance for uncoded theoretical and coded simulation scenarios. Due to the more severe fading present in the coded simulation scenario, the modulation order is more quickly reduced; however, when this happens, in both scenarios the number of hops grows in order to reduce the overall energy consumption. In addition, the Table 5 presents the optimal parameters for each link distance, including the optimal code rate employed in simulations.

Figure 20 – Total energy consumption for the coded case comparison as a function of the link distance.

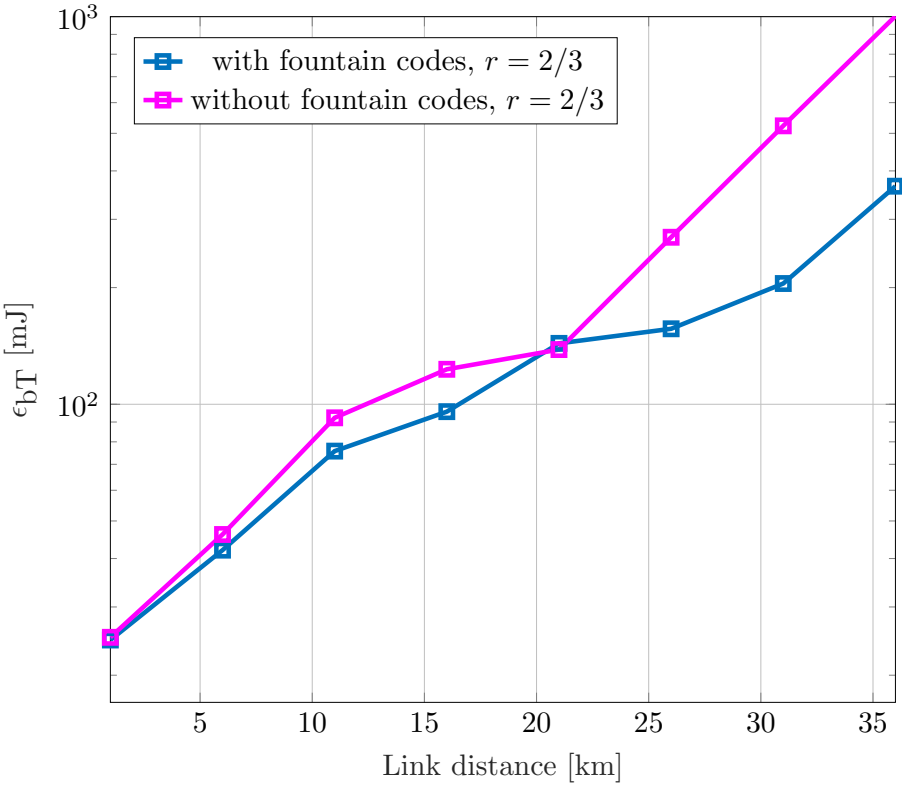

Source: The Author.

Table 5 – Optimal parameters

Distance [km]	$M_{\mathbf{opt,uncoded}}$	$\varphi_{\mathbf{opt,uncoded}}$	$M_{\text{opt,coded}}$	$\varphi_{\mathbf{opt,coded}}$
1	16	1	16	1
6	16	1	8	1
11	16	2	8	2
16	16	2	8	2
21	16	3	4	2
26	8	3	4	3
31	4	3	4	3

Source: The Author.

Figure 21 – Number of packets encoded by the fountain code Y as a function of the link distance for 16-DPSK.

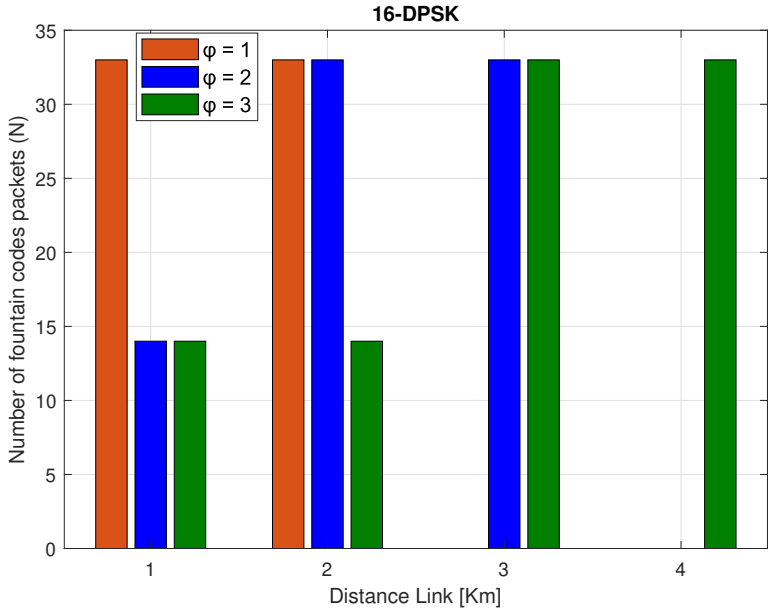

Source: The Author.

Finally, Figure 21 shows the number of encoded packets Y by fountain codes for a minimum value of packets $Z = 10$, for different number of hops φ, $\tau = 1$ and $M = 16$ as a function of the link distance. The behavior of simulation and numerical results is the same. The number of extra packets Y considerably increases with the distance, and transmissions using higher modulations order require more packets to successfully reach the target FER and the saturation effect is reached easily. When increasing the number of hops, Y takes longer to reach saturation. Nevertheless, we notice a quantitative difference between theoretical and simulation results, which occurs due to the more complete scenario used in the simulations, including the K-fading and the convolutional encoding.

5 CONCLUSIONS

In this document, we have analyzed the energy consumption of underwater acoustic networks employing fountain codes in different scenarios in order to explore the main problem found in this context: the high energy consumption. We consider the optimization of the number of hops, retransmissions and the modulation order to obtain the lowest possible energy consumption. We also have investigated the impact of optimizing each parameter separately in this process. Therefore, first we model the underwater channel according to the characteristics of the attenuation, noise, SNR, fading and error probability. Moreover, we consider fountain codes and retransmissions. Then, we propose a optimization of system parameters in order to meet a given target FER. In additional, we present the proposal of an algorithm to optimize the number of fountain packets, where the main goal is the minimization of the number of fountain packets, while maintaining a valid SNR for transmission. Finally, the energy consumption model is presented, where the fountain codes, retransmissions and multiple-hops are considered.

Our theoretical analysis, validated by numerical and simulation results, indicates that optimizing the number of hops, allowing retransmission and employing fountain codes is fundamental to minimize the energy consumption for medium to long links, while optimizing the modulation order has a smaller impact in terms of energy savings.

For future studies, we suggest studying optimization techniques for orthogonal frequency division multiplexing (OFDM) systems focusing on energy efficiency, which is under explored in underwater scenarios due to the complexity of this approach. However, some studies indicate that this approach may be interesting both to improve performance and energy savings.

For instance, in (ZHAO et al., 2017) a carrier aggregation in OFDM-based underwater acoustic cellular networks was proposed, which the communication rate and energy efficiency are evaluated via simulations and experiments. The carrier aggregation technique improves the total throughput of OFDM using an expanded bandwidth, where multiple carriers are aggregated for data transmission from one transmitter. The results indicate that carrier aggregation can greatly improve the achievable underwater communication rate for distances up to 5 km. Moreover, it was noticed that the maximum bandwidth configuration does not achieve the optimal energy efficiency. However, there is an optimal bandwidth that can lead to such optimal energy efficiency.

A recent and very promising line of study is the use of Machine Learning in UWANs. The underwater environment is very dynamic, so developing algorithms that learn from the channel can be very interesting. In addition, the optimization of parameters based on real measurements can further improve results. In (JAHANBAKHT et al., 2021) some applications are presented where machine learning is already being used in underwater environments, as seabed analysis and mapping, object classification and discovery, plant identification, automatic recognition of fish, fish farming, pipeline monitoring and corrosion investigation, etc.

Another promising line of studies reported in UWANs is Edge Computing (JAHANBAKHT et al., 2021), where the endpoint (edge) devices perform all or part of the required computations, so the need for data transfer and communication becomes less of a challenge. That is, this would reduce the number of hops, considerably changing the energy efficiency optimization performed. Also, other advantages of using such a decentralized edge computing technology in UWANs are data-rate reduction, latency reduction, and prompt inner-network decisions making.

REFERENCES

AHMED, M. S. R. Joint power and rate control for packet coding over fading channels. **IEEE JOURNAL OF OCEANIC ENGINEERING, VOL. 42, NO. 3,**, 2017.

AOUAMI, R.; RIFI, M.; OUZZIF, M. Improve the energy efficiency in wireless sensor networks fountain code theory. **Information Technology, Electronics and Mobile Communication Conference (IEMCON), 2017 8th IEEE Annual**, 2017.

BARRETO, G. et al. Energy-efficient channel coding strategy for underwater acoustic networks. **Sensors (Basel), 17(4), 728**, 2017.

BARRETO, G. et al. Energy-efficient channel coding strategy for underwater acoustic networks. **Sensors**, Multidisciplinary Digital Publishing Institute, v. 17, n. 4, p. 728, 2017.

BEGIN, G.; HACCOUN, D.; PAQUIN, C. Further results on high-rate punctured convolutional codes for Viterbi and sequential decoding. **IEEE Trans. Commun.**, v. 38, n. 11, p. 1922–1928, Nov 1990. ISSN 0090-6778.

CHEN, W. et al. Reliable and opportunistic transmissions for underwater acoustic networks. **IEEE Network**, IEEE, v. 32, n. 4, p. 94–99, 2018.

CHEN, X.; SUBRAMANIAN, V. G.; LEITH, D. J. Phy modulation/rate control for fountain codes in 802.11 a/g wlans. **Physical Communication**, Elsevier, v. 9, p. 135–144, 2013.

EVOLOGICS. **S2C R 48/78 Underwater Acoustic Modem**. 2018. Disponível em: https://evologics.de/acoustic-modem/48-78/r-serie.

FREITAG, L. et al. The WHOI micro-modem: an acoustic communications and navigation system for multiple platforms. In: **IEEE OCEANS Conf**. 2005.

GAO, M.; FOH, C. H.; CAI, J. On the selection of transmission range in underwater acoustic sensor networks. **Sensors**, v. 12, n. 4, p. 4715–4729, 2012. ISSN 1424-8220.

GRADSHTEIN, I.; RYZHIK, I.; JEFFREY, A. **Table of Integrals, Series, and Products**. 7th. ed. Academic Press, 2000. ISBN 9780122947575.

HEIDEMANN, J. et al. Research challenges and applications for underwater sensor networking. In: **IEEE Wireless Communications and Networking Conference (WCNC)**. 2006. v. 1, p. 228–235. ISSN 1525-3511.

JAHANBAKHT, M. et al. Internet of underwater things and big marine data analytics—a comprehensive survey. **IEEE COMMUNICATIONS SURVEYS & TUTORIALS**, v. 23, n. 2, 2021.

JIANG, S. On reliable data transfer in underwater acoustic networks: A survey from networking perspective. **IEEE Communications Surveys & Tutorials**, 2018.

LIANG, M.; DUAN, J.; ZHAO, D. Optimal redundancy control strategy for fountain code-based underwater acoustic communication. **IEEE Access**, IEEE, v. 6, p. 69321–69334, 2018.

LIVA, G.; PAOLINI, E.; CHIANI, M. Performance versus overhead for fountain codes over Fq. **IEEE Commun. Lett.**, v. 14, n. 2, p. 178–180, Feb. 2010.

MOHAMMADI, Z. et al. Increasing the lifetime of underwater acoustic sensor networks: Difference convex approach. **IEEE SYSTEMS JOURNAL**, v. 14, n. 3, set. 2020.

PROAKIS, J.; SALEHI, M. **Digital Communications**. McGraw-Hill, 2001. ISBN 9780072321111.

RAMEEZ, A.; STOJANOVIC, M. Random linear packet coding for fading channels. **OCEANS - San Diego**, n. 1-6, 2013.

ROSAS, F.; OBERLI, C. Modulation and SNR optimization for achieving energy-efficient communications over short-range fading channels. **IEEE Trans. Wireless Commun.**, v. 11, n. 12, p. 4286–4295, Dec. 2012. ISSN 1536-1276.

SIGNORI, A. et al. A game-theoretic and experimental analysis of energy-depleting underwater jamming attacks. **IEEE INTERNET OF THINGS JOURNAL**, v. 7, n. 10, out. 2020.

SIMAO, D. et al. Energy consumption analysis of underwater acoustic networks using fountain codes. **MTS/IEEE Oceans'16, Monterrey**, 2016.

SIMAO, D. et al. Energy efficiency of multi-hop underwater acoustic networks using fountain codes. **IEEE Access**, v. 8, p. 23110 – 23119, jan. 2020.

SONG, Y. Underwater acoustic sensor networks with cost efficiency for internet of underwater things. **IEEE TRANSACTIONS ON INDUSTRIAL ELECTRONICS**, v. 68, n. 2, fev. 2021.

SOUZA, F. et al. Optimizing the number of hops and retransmissions for energy efficient multi-hop underwater acoustic communications. **IEEE SENSORS JOURNAL**, v. 16, n. 10, p. 3927–3938, 2016.

SOUZA, F. et al. Modulation order optimization for energy efficient underwater acoustic communications. **MTS/IEEE Oceans'16, Monterrey**, 2016.

SOUZA, F. A. et al. Code rate optimization for energy efficient delay constrained underwater acoustic communications. **Oceans - Genova**, 2015.

SRIVASTAVA, R.; KOKSAL, C. E. Energy optimal transmission scheduling in wireless sensor networks. **IEEE Transactions on Wireless Communications**, v. 9, n. 5, p. 1550–1560, May 2010. ISSN 1558-2248.

STOJANOVIC, M. On the relationship between capacity and distance in an underwater acoustic communication channel. In: **1st ACM Int. Workshop on Underwater Netw.** New York, NY, USA, 2006. p. 41–47. ISBN 1-59593-484-7.

TOMASI, B.; PREISIG, J. C. Energy-efficient transmission strategies for delay constrained traffic with limited feedback. **IEEE Transactions on Wireless Communications**, v. 14, n. 3, p. 1369–1379, March 2015. ISSN 1558-2248.

TOMASI, B.; PREISIG, J. C. Evaluating energy-efficient schedulers on underwater acoustic data. In: **OCEANS 2019 - Marseille**. 2019. p. 1–7. ISSN null.

XING, C. T. Y. Dynamic fountain codes for energy efficient data dissemination in underwater sensor networks. In: **IEEE OCEANS - Anchorage**. 2017.

YANG, W.-B.; YANG, T. C. M-ary frequency shift keying communications over an underwater acoustic channel: Performance comparison of data with models. **J. Acoustical Society of America**, v. 120, n. 5, p. 2694–2701, 2006.

YILDIZ, H. Maximization of underwater sensor networks lifetime via fountain codes. **IEEE Transactions on Industrial Informatics**, 2019.

ZHAO, X.; POMPILI, D.; ALVES, J. Underwater acoustic carrier aggregation: Achievable rate and energy-efficiency evaluation. **IEEE JOURNAL OF OCEANIC ENGINEERING, VOL. 42, NO. 4**, 2017.

ZHOU, J.-H. C. . J. K. . M. G. . S. The challenges of building scalable mobile underwater wireless sensor networks for aquatic applications. **IEEE Network**, v. 20, p. 12–18, 2006.